Noble gas and oxygen isotope studies of aubrites: a clue to origin and histories

Yayoi N. MIURA[1*], Hiroshi HIDAKA[2],

Kunihiko NISHIIZUMI[3] and Minoru KUSAKABE[4]

[1] Earthquake Research Institute, University of Tokyo, 1-1-1 Yayoi, Bunkyo-ku, Tokyo 113-0032, Japan

[2] Department of Earth and Planetary Systems Science, Hiroshima University, Higashi-Hiroshima, Hiroshima 739-8526, Japan

[3] Space Science Laboratory, University of California, Berkeley, Berkeley, CA 94720-7450, U.S.A.

[4] Institute for Study of the Earth's Interior, Okayama University, Misasa, Tottori 682-0193, Japan

Abstract – Noble gas measurements were performed for nine aubrites: Bishopville, Cumberland Falls, Mayo Belwa, Mt. Egerton, Norton County, Peña Blanca Spring, Shallowater, ALHA 78113 and LAP 02233. These data clarify the origins and histories, particularly cosmic-ray exposure and regolith histories, of the aubrites and their parent body(ies). Accurate cosmic-ray exposure ages were obtained using the ^{81}Kr-Kr method for three meteorites: 52 ± 3, 49 ± 10 and 117 ± 14 Ma for Bishopville, Cumberland Falls and Mayo Belwa, respectively. Mayo Belwa shows the longest cosmic-ray exposure age determined by the ^{81}Kr-Kr method so far, close to the age of 121 Ma for Norton County. These are the longest ages among stony meteorites. Distribution of cosmic-ray exposure ages of aubrites implies 4-9 break-up events (except anomalous aubrites) on the parent body. Six aubrites show "exposure at the surface" on their parent body(ies): (i) neutron capture ^{36}Ar, ^{80}Kr, ^{82}Kr and/or ^{128}Xe probably produced on the respective parent body (Bishopville, Cumberland Falls, Mayo Belwa, Peña Blanca Spring, Shallowater and ALHA 78113); and/or (ii) chondritic trapped noble gases, which were likely released from chondritic inclusions preserved in the aubrite hosts (Cumberland Falls, Peña Blanca Spring and ALHA 78113). The concentrations of ^{128}Xe from neutron capture on ^{127}I vary among four measured specimens of Cumberland Falls (0.5-76 × 10^{-14} cm^{3}STP/g), but are correlated with those of radiogenic ^{129}Xe, implying that the concentrations of $(^{128}Xe)_n$ and $(^{129}Xe)_{rad}$ reflect variable abundances of iodine among specimens. The ratios of $(^{128}Xe)_n/(^{129}Xe)_{rad}$ obtained in this work are different for Mayo Belwa (0.045), Cumberland Falls (0.015), and Shallowater (0.001), meaning that neutron fluences, radiogenic ^{129}Xe retention ages, or both, are different among these aubrites. Shallowater contains abundant trapped Ar, Kr and Xe (2.2 × 10^{-7}, 9.4 × 10^{-10} and 2.8 × 10^{-10} cm^{3}STP/g, respectively) as reported previously (Busemann and Eugster, 2005, *MAPS* **37**, 1865-1891). Isotopic compositions of Kr and Xe in Shallowater are consistent with those of Q (a primordial noble gas component trapped in chondrites). The Ar/Kr/Xe compositions are somewhat fractionated from Q, favoring lighter elements. Because of the unbrecciated nature of Shallowater, Q-like noble gases are considered to be primordial in origin. Fission Xe is found in Cumberland Falls, Mayo Belwa, Peña Blanca Spring, ALHA 78113 and LAP 02233. The majority of fission Xe is most likely ^{244}Pu-derived, and about 10-20% seems to be ^{238}U-derived at ^{136}Xe. The observed $(^{136}Xe)_{Pu}$ corresponds to 0.019-0.16 ppb of ^{244}Pu, from which the ^{244}Pu/U ratios are calculated as 0.002-0.009. These ratios resemble

those of chondrites and other achondrites like eucrites, suggesting that no thermal resetting of the Pu-Xe system occurred after ~4.5 Ga ago. We also determined oxygen isotopic compositions for four aubrites with chondritic noble gases and a new aubrite LAP 02233. In spite of their chondritic noble gas signatures, oxygen with chondritic isotopic compositions was found only in a specimen of Cumberland Falls ($\Delta^{17}O$ of ~0.3‰). The other four aubrites and the other two measured specimens of Cumberland Falls are concurrent with the typical range for aubrites.

1. INTRODUCTION

Aubrites (enstatite achondrites) are composed of nearly Fe-O free enstatite with rare minerals formed under highly reducing conditions (e.g., Watters and Prinz, 1979; Rubin, 1983; Okada et al., 1988; Keil, 1989). A close relationship between aubrites and enstatite chondrites (sub-divided into EL and EH groups) has been suggested from mineralogical, chemical and oxygen isotope investigations. For oxygen isotopic compositions, aubrites and enstatite chondrites, except Cumberland Falls, reveal a common mass fractionation trend that is consistent with the terrestrial mass fractionation line (Clayton et al., 1984; Clayton, 1993; Newton et al., 2000), indicating that aubrites, enstatite chondrites and the Earth were produced from a reservoir with a single oxygen isotopic composition. Aubrites are thought to have been formed through an igneous differentiation process of enstatite chondrite-like material. However, a comprehensive formation scenario has not been presented. Among meteorites classified as aubrites, Mount Egerton, Queen Alexandra Range (QUE) 97289/97348 and Shallowater were recognized as unusual, due to differences in mineralogy and chemistry from the other aubrites (Watters and Prinz, 1979; Keil et al., 1989; Antarctic Meteorite Newsletter, 1999, 22 (1); Antarctic Meteorite Newsletter, 2000, 23 (1)). Only these aubrites are unbrecciated: the others are regolith or fragmental breccias. Shallowater was inferred to have a complex formation history, an igneous process followed by impact, and to have originated from a parent body different from other aubrites (Keil et al., 1989). Mt. Egerton shows a higher metal content. It was suggested that this aubrite may be a sample of the mantle-core boundary of the aubrite parent body (Watters and Prinz, 1979).

A remarkable feature is that about one-third of all aubrites contain implanted solar wind (SW) noble gases. Mathew and Marti (2003) showed that the isotopic composition of SW Xe in the aubrite Pesyanoe resembles that in lunar regolith samples, indicating that SW Xe compositions were the same at two distinct solar system locations in different epochs. A distinct property of aubrites is the range of cosmic-ray exposure ages. Lorenzetti et al. (2003) compiled noble gas data (He, Ne and Ar for 22 aubrites from their measurements and literature), based on which they suggested that aubrites have various cosmic-ray exposure ages from 13 to 116 Ma with some remarkable peaks in the age distribution around

15, 23 and 56 Ma. The members of the 15 and 23 Ma groups are mostly Allan Hills aubrites; the data do not rule out that all are paired. They pointed out that, if these are pairs, it is necessary to explain the difference using a model of regolith evolution and precompaction irradiation for the aubrites with the longer exposure ages of ~23 Ma. Although the ^{81}Kr-Kr method is a good technique for accurate exposure age determinations, only one aubrite has been determined so far (52 ± 17 Ma for Khor Temiki by Eugster et al., 1969) due to the very low abundances of ^{81}Kr. Furthermore, Kr produced from neutron captures on Br was discussed by Lorenzetti et al. (2003), who reported considerable amounts of $(^{80}Kr)_n$ and $(^{82}Kr)_n$ in four aubrites. Combining this with results given by Hidaka et al. (1999) showing Sm and Gd isotope shifts due to neutron capture, Lorenzetti et al. (2003) suggested that neutron capture Kr is from a pre-irradiation occurring on the parent asteroid. Complete noble gas results were given for about seven aubrites in other studies (Rowe and Bogard, 1966; Eugster et al., 1969; Kim and Marti, 1992; Busemann and Eugster, 2002; Lorenzetti et al., 2003; Mathew and Marti, 2003). However, the details of trapped noble gas components were studied only for Pesyanoe, which contains SW noble gases (Kim and Marti, 1992; Mathew and Marti, 2003).

In the present study, noble gas measurements were made for nine aubrites: Bishopville, Cumberland Falls, Mayo Belwa, Mount Egerton, Norton County, Peña Blanca Spring, Shallowater, Allan Hills (ALH) A 78113 and LaPaz Ice Field (LAP) 02233. These measurements were used to clarify cosmic-ray exposure and regolith histories and to provide constraints on the origin and evolution of aubrite parent body(ies). The ^{81}Kr-Kr ages were determined for three of them in this work. In addition to noble gas measurements, we also performed oxygen isotope measurements for five aubrites, four aubrites with chondritic noble gas signatures and one newly found aubrite LAP 02233.

2. SAMPLES AND EXPERIMENTAL METHODS

2.1. Samples

We obtained several samples from different sources for Cumberland Falls, Norton County and

Peña Blanca Spring. These might have had different shielding conditions, although the position within the meteoroid is not known for any sample. The obtained samples are interior chips without fusion crust (exceptions are fine grained samples for Bishopville and Shallowater), and were crushed to smaller grain sizes for noble gas and oxygen measurements. For noble gas measurements, we used samples that had been broken to grain sizes < 500 μm for Cumberland Falls #3 and Peña Blanca Spring #3 and #4, and larger grains of a few millimeters for the others. For oxygen isotope measurements, several small grains were crushed with an agate mortar to smaller sizes. Noble gas analyses for two specimens taken from single cm-sized fragments were made on four aubrites (Table 1). For these samples, noble gas variations are likely to reflect chemical heterogeneity or processes on parent body. No measured aubrites contain solar noble gases.

Some samples used in this work were also used for collaborative investigations on neutron capture Sm and Gd isotopes and cosmogenic radionuclides. A specimen was separated from common pieces for the following samples: Cumberland Falls #3, Norton County #3, Peña Blanca Spring #3 and #4 and Shallowater #1 for Sm and Gd isotopic studies (Hidaka et al., 1999; Hidaka et al., 2003; Hidaka et al., 2006) and Cumberland Falls #1 and #2, Mayo Belwa #1, Mt. Egerton #1 and #2, Norton County #1 and #2 and Peña Blanca Spring #1 and #2 for cosmogenic radionuclide studies (Welten et al., 2002; Welten et al., 2004).

2.2 Noble gas analysis

Noble gases were measured with a mass spectrometer at the Laboratory for Earthquake Chemistry, University of Tokyo. The analytical procedure basically resembles our standard one for meteorite analyses (e.g., Miura et al., 1995; Nagao et al., 1999). For gas extraction, we used conventional step-heating. In addition, gas extraction using a vacuum crusher technique was applied before step-heating for some samples. The crusher system used in this work (e.g. Okazaki et al., 2003) enables gas extraction by crushing and heating without exposure to the terrestrial atmosphere. It presents advantages for research on trapped noble gases existing in bubbles and eliminates adsorption of terrestrial atmosphere onto the fresh

surface that was made during crushing. Conditions of gas extraction for the measured samples are shown in Table 1 and in electronic annex EA-1.

Each aubrite sample, weighing 0.02-0.40 g, was wrapped in Aluminum foil. The sample was loaded into a glass sample holder (heating only) or into a stainless steel line (crushing and heating). The sample storage area was pre-heated overnight at ~150°C under ultra-high vacuum. For samples analyzed by heating only, noble gases were extracted in a Mo crucible either in a single step at 1700°C (for Mt. Egerton #1), two-steps at 600 and 1800°C (for 13 analyses), or four-steps at 600, 1000, 1400 and 1800°C (for Mt. Egerton #2). In the crushing method, samples were struck in a Mo crucible ~500 times with a stainless steel pestle. This crushing process was repeated three times. On each occasion, released noble gases were measured. After crushing, a four-step heating in the same Mo crucible was applied. Extracted gases were purified with two Ti-Zr getters and two Sorb-AC getters to remove active gases. Noble gases were separated cryogenically into four fractions, He-Ne, Ar, Kr, and Xe, each of which was admitted into a modified-VG5400 mass spectrometer. All stable noble gas isotopes and ^{81}Kr (half life = 2.3×10^5 years) were analyzed using a computer-controlled peak jumping method. Although ^{81}Kr was analyzed in all samples except Cumberland Falls #4 and Peña Blanca Spring #5, detection was successful for only some samples because of low abundances of ^{81}Kr. We monitored crushing and heating blanks before sample measurements. Vacuum crushing blanks for ^{4}He, ^{20}Ne, ^{36}Ar, ^{84}Kr and ^{132}Xe are (2-4) $\times 10^{-12}$, (4-8) $\times 10^{-13}$, (1-3) $\times 10^{-12}$, (5-12) $\times 10^{-14}$ and (1-2) $\times 10^{-14}$ cm^{3}STP/g, and heating blanks at 1800°C are (1-100) $\times 10^{-11}$, (1-8) $\times 10^{-12}$, (2-8) $\times 10^{-12}$, (3-30) $\times 10^{-14}$ and (0.3-20) $\times 10^{-14}$ cm^{3}STP/g, respectively. All data shown in this paper represent results after blank and mass discrimination corrections.

2.3. Oxygen isotope analysis

Oxygen isotopes were measured with the CO_2 laser-BrF_5 fluorination technique at the Institute for Study of the Earth's Interior, Okayama University. The system and technical details were given in Kusakabe et al. (2004). Overnight evacuation of the samples at ~180°C, followed by pretreatment by BrF_5 (100 hPa) for up to several hours, was done to remove contamination by atmospheric moisture. For

extraction of oxygen by fluorination, the sample was irradiated using a CO_2 laser under ~1.2×10^4 Pa BrF_5 atmosphere. The liberated O_2 gas, which was purified through several cryogenic traps and a KBr trap (150°C), was finally collected onto a cold finger containing a Molecular Sieve 13X that was attached next to a micro-inlet of an isotope ratio mass spectrometer equipped with a dual-inlet and triple collector (SIRA12, Micromass, UK). High purity O_2 gas calibrated against the VSMOW-SLAP scale (Gonfiantini et al., 1995) was used as a working standard to obtain $\delta^{17}O$ and $\delta^{18}O$ values on the SMOW scale. The analytical accuracy of the $\delta^{17}O$ and $\delta^{18}O$ measurements is approximately 0.1‰.

3. RESULTS AND DISCUSSION

3.1. Oxygen isotopic compositions as a clue to the origin of a chondritic noble gas signature in aubrites

Results for oxygen isotopes are given in Table 2 and Fig. 1. Deviation from the terrestrial mass fractionation line is calculated from the equation $\Delta^{17}O = \delta^{17}O - 0.52 \times \delta^{18}O$ (Clayton, 1993). Previous work revealed that most aubrites plot on the terrestrial mass fractionation trend ranging from 4.5 to 5.8‰ in $\delta^{18}O$ (Clayton and Mayeda, 1996; Newton et al., 2000) and that the averaged $\Delta^{17}O$ of aubrites is 0.02 ± 0.04‰ (calculated from 13 samples by Clayton and Mayeda, 1996) and -0.022 ± 0.048‰ (from eight samples by Newton et al., 2000). Four aubrites studied in this work, Peña Blanca Spring, Shallowater, ALHA 78113 and LAP 02233, lie on the terrestrial mass fractionation line within experimental error. Among three analyses of Cumberland Falls, one sample showed a high $\Delta^{17}O$ of 0.34‰; the other two samples showed usual aubritic compositions, $\Delta^{17}O$ being -0.06 and 0.00‰ (Table 2). Clayton et al. (1984) reported a normal aubritic oxygen isotopic composition of 0.07‰ in $\Delta^{17}O$ (2.76‰ in $\delta^{17}O$ and 5.18‰ in $\delta^{18}O$) for a bulk sample of Cumberland Falls, whereas Verkouteren and Lipschutz (1983) reported those with a high $\Delta^{17}O$ of 0.93‰ for a chondritic clast in Cumberland Falls. The clast was proposed to have LL chondrite affinity based on the mineralogy and oxygen isotope compositions. Newton et al. (2000) reported $\Delta^{17}O$ of 0.53‰ for a bulk sample of Cumberland Falls, and suggested that 60% of the oxygen

was from LL chondrite material assuming that the chondritic inclusions had $\Delta^{17}O$ of 0.93‰. From previous and present results showing various $\Delta^{17}O$ values among measured specimens, LL (or possibly L) chondritic materials are likely incorporated into the aubrite host in a fine and heterogeneous fashion. This interpretation is consistent with the fact that the amounts of chondritic noble gases are also widely variable within the measured specimens of Cumberland Falls. Previous studies have also found slightly high $\Delta^{17}O$ of ALHA 78113 (0.08 and 0.09‰, respectively, by Clayton and Mayeda, 1996 and Newton et al., 2000). Reportedly, ALHA 78113 contains chondritic inclusions (Lipschutz et al., 1988). Some data for ALHA 78113 and Peña Blanca Spring measured in this work show similarly high $\Delta^{17}O$ (0.06-0.12‰). Although these values are not much greater than the experimental uncertainties in the present study, these might be signatures for incorporation of chondritic inclusions. Both aubrites released chondritic trapped noble gases, which will be discussed later. Oxygen contents in aubrites and chondrites are similar, but primordial noble gas abundances in chondrites are higher than those in aubrites, which results in more efficient detection of chondritic components by measure of primordial noble gases rather than oxygen. LAP 02233, which does not have a chondritic trapped noble gas signature, gives 0.06‰ in $\Delta^{17}O$ for the two measured samples, which is the typical oxygen isotope composition of aubrites within error.

3.2. Overview of noble gas results and decomposition into components

Table 1 shows noble gas results, calculated as totals from crushing and heating steps. The complete noble gas data for all extraction steps are given in electronic annex EA-1. Isotopic ratios of He and Ne indicate that He and Ne is dominated by a cosmogenic component. The $^{3}He/^{4}He$ ratios of Mt. Egerton, Norton County #1 and #2, Peña Blanca Spring #1 and #3 and Shallowater are close to the pure cosmogenic He ratios for stony meteorites of ~ 0.20. For the other samples, $^{3}He/^{4}He$ is somewhat lower because of the contribution of radiogenic ^{4}He. For Ne, only Ne at 600°C of Mt. Egerton #2 shows a large contribution of trapped Ne, which seems to originate from terrestrial atmospheric contamination. The measured $^{38}Ar/^{36}Ar$ ratios show that Ar is a mixture of trapped and cosmogenic Ar, except in Shallowater. The $^{38}Ar/^{36}Ar$ ratio of Shallowater is 0.1865±0.0004, which we consider to represent the isotopic

composition of Q-Ar ($^{38}Ar/^{36}Ar$ = 0.1872; Ott, 2002). Radiogenic ^{40}Ar is contained in all measured aubrites.

Both Kr and Xe are mixtures of several components: trapped, cosmogenic, neutron-capture-produced and fission-derived components. We separated the measured Kr and Xe in aubrites into individual components, basically following a technique that is often used for achondrites (Eugster and Michel, 1995; Miura et al., 1998; Busemann and Eugster 2002). The mixing ratios of trapped and cosmogenic components were determined assuming (i) ^{83}Kr and ^{86}Kr consists of cosmogenic, trapped and fission Kr (fission is only at ^{86}Kr) and (ii) ^{126}Xe and ^{130}Xe consists of cosmogenic and trapped Xe. The concentrations of fission ^{86}Kr were calculated based on ^{238}U and ^{244}Pu abundances, for which U contents reported and ^{244}Pu contents determined based on $(^{136}Xe)_{Pu}$ were used. The contribution of $(^{86}Kr)_f$ is usually < 0.1% in most samples, but exceptions exist with the highest contribution being 2.0% for the 1400°C step from Cumberland Falls #2. After the trapped-cosmogenic separation mentioned above, the isotopic spectra of trapped and cosmogenic Kr and Xe listed below were assumed for evaluating the amounts of Kr and Xe produced from neutron capture, radiogenic ^{129}Xe, and fission $^{131\text{-}136}Xe$. For trapped Kr and Xe, we used the isotopic ratios of terrestrial atmosphere or Q according to the observed $^{36}Ar/^{84}Kr/^{132}Xe$ elemental compositions in each extraction step of each sample (cf., Section 3.8). Note that the mass-dependent fractionation in isotopic compositions is considered to be very small based on the degree of elemental fractionation. The ratios for terrestrial atmospheric Kr and Xe were taken from Ozima and Podosek (2002), and those for Q-Kr and Q-Xe from Busemann et al. (2000). The empirical composition determined for aubrites by Lorenzetti et al. (2003) was adopted for cosmogenic Kr, whereas the composition of cosmogenic Xe as calculated for aubritic chemical compositions (Busemann et al., 2000) or for a Ba target (Hohenberg et al., 1981) was used: $(^{80}Kr/^{83}Kr)_c$=0.560, $(^{82}Kr/^{83}Kr)_c$=0.764, $(^{86}Kr/^{83}Kr)_c$=0.015, $(^{128}Xe/^{126}X)_c$=1.5 or 1.621, $(^{129}Xe/^{126}X)_c$=1.6, $(^{130}Xe/^{126}X)_c$=1 or 1.248, $(^{131}Xe/^{126}X)_c$=3.9 or 4.36, $(^{132}Xe/^{126}X)_c$=0.9 or 1.053, $(^{134}Xe/^{126}X)_c$=0 or 0.069, and $(^{136}Xe/^{126}X)_c$=0 or 0.004. Decomposition of Xe using the cosmogenic Xe calculated for aubritic chemical compositions shows no internal consistency in some measured aubrites; the use of cosmogenic Xe for Ba target seems to be plausible for them. We chose either cosmogenic spectrum according to isotope plots like $^{124}Xe/^{130}Xe$ vs. $^{126}Xe/^{130}Xe$ (cf., Section 3.6).

For decomposition of Ar, excepting 1800°C of Shallowater, $(^{38}Ar/^{36}Ar)_t$=0.188 and $(^{38}Ar/^{36}Ar)_c$=1.55 were used, respectively, for trapped and cosmogenic Ar.

3.3. Terrestrial atmospheric noble gas contribution and noble gases released in crushing steps

Bishopville, Mt. Egerton #2, Norton County #1 and ALHA 78113 released more ^{36}Ar, ^{84}Kr and ^{132}Xe at 600°C than at higher temperatures. These noble gases are likely terrestrial atmospheric noble gases, as inferred from their low release temperature and their noble gas elemental and isotopic compositions. The measured specimen of Mt. Egerton appeared to be highly weathered. During weathering on the Earth, terrestrial atmospheric noble gases probably were incorporated into secondary minerals. Other samples might have also been affected by the same process. The terrestrial atmospheric noble gases were released even at high temperature steps. For example, the 1800°C step of Norton County #2 agrees well with terrestrial atmospheric elemental and isotopic compositions (elemental compositions are mass fractionated patterns of the terrestrial atmosphere), indicating that the terrestrial atmospheric noble gases were retained up to above 1400°C. Processes for the terrestrial noble gas uptake in meteorites and lunar samples have been studied by several investigators (e.g., Yang et al., 1982; Wacker et al., 1985; Bogard et al., 1989), but no conclusive mechanism has been recognized. One plausible phenomenon aside from trapping during production of secondary minerals is the implantation of adsorbed noble gases on grain surfaces during sample preparation (Niedermann and Eugster, 1992), which explains releases at high temperatures and the mass fractionated terrestrial noble gas patterns favoring heavier elements as observed in the aubrite samples.

The release profiles of ^{84}Kr and ^{132}Xe in Norton County #2 are quite similar to those in Cumberland Falls #2. However, only sample Cumberland Falls #2 shows characteristics of chondritic noble gases (here we use the term "chondritic noble gas" in a broad sense: noble gases showing elemental compositions like Q, solar, Ar-rich or mass fractionation of them, which we will discuss in section 3.8). Similarly, although the ^{132}Xe release profiles are similar between Norton County #2 and Peña Blanca Spring #2, only Peña Blanca Spring #2 released chondritic noble gases at high temperatures. It is difficult

to evaluate noble gas components or origins in the aubrite samples based only on release temperatures and profiles.

Crushing experiments release primarily noble gases from voids and fragile phases rather than in-situ produced noble gases such as cosmogenic and nucleogenic ones residing within minerals (e.g. in solid-phase lattice defects). Although we expected primordial noble gases to be released preferentially in crushing experiments from microscopic voids that might have been formed during crystallization, only terrestrial atmospheric noble gases were released in crushing steps. Even Cumberland Falls #2 and Peña Blanca Spring #2, which released chondritic noble gases in heating steps, released noble gases with terrestrial atmospheric compositions in crushing steps. This release behavior indicates that chondritic noble gases are never trapped in void or fragile phases in aubrites. Crushing steps release a higher fraction of terrestrial atmospheric noble gases (Ar, Kr and Xe) than cosmogenic gases (He, Ne and Ar), from which we suppose that the terrestrial atmospheric Ar, Kr and Xe is trapped near grain surfaces rather than in the interior, and that it was efficiently released by destruction of surface layers during crushing rather than at low temperature steps because of a large desorption energy. A more complete explanation of release profiles and terrestrial atmospheric noble gases is given in electronic annex EA-2.

3.4. Cosmogenic noble gases and production rates

Neon with low $^{20}Ne/^{22}Ne$ and $^{21}Ne/^{22}Ne$ ratios was released at the lowest temperature step, 600°C, of Bishopville, Mayo Belwa and Peña Blanca Spring #5 (Table EA-1-1 in EA-1). The respective $^{20}Ne/^{22}Ne$ and $^{21}Ne/^{22}Ne$ ratios are 0.658 and 0.713 for Bishopville, 0.689 and 0.750 for Mayo Belwa and 0.713 and 0.714 for Peña Blanca Spring #5, which closely resemble those of cosmogenic Ne observed in Na-rich oligoclase feldspar (0.5-0.7 and ~0.7 for $^{20}Ne/^{22}Ne$ and $^{21}Ne/^{22}Ne$, respectively; Smith and Huneke, 1975). The production of ^{22}Ne is enhanced in Na-rich minerals through the reaction chain ^{23}Na (n, 2n) $^{22}Na \rightarrow {}^{22}Ne$. High Na contents were reported for Bishopville and Mayo Belwa (0.54 and 0.95%), whereas Peña Blanca Spring contains a moderate Na concentration of 0.28% (Lorenzetti et al., 2003). These Na contents can explain the observed low $^{21}Ne/^{22}Ne$ ratios assuming Ne production rates reported in literature (Smith

and Huneke, 1975). This calculation is shown in electronic annex EA-3.

The concentrations of cosmogenic noble gases are presented in Table 3. In contrast to those of cosmogenic ^{3}He and ^{21}Ne, the concentrations of cosmogenic ^{38}Ar, ^{81}Kr, ^{83}Kr and ^{126}Xe are variable within a single aubrite. We will discuss cosmic-ray exposure ages based on ^{3}He, ^{21}Ne, and ^{81}Kr-Kr, a method not sensitive to target element compositions. For production rates of cosmogenic ^{3}He and ^{21}Ne (P_3 and P_{21}), we basically use equations for P_3 proposed for chondrites (Eugster, 1988) and for P_{21} for aubrites (Lorenzetti et al., 2003). The equation for P_3 is $P_3 = F_3$ (2.09 – 0.43 $(^{22}Ne/^{21}Ne)_c$), where F_3 is the "chemical composition factor relative to L chondrite; P'_3 (aubrite sample) / P'_3 (L chondrite)" and $(^{22}Ne/^{21}Ne)_c$ is the cosmogenic ^{22}Ne/^{21}Ne ratio of the sample as a parameter of shielding. $P'_3 = 1.74$ [Ti + Cr + Mn + Fe + Ni] + 2.66 (100 - [Ti + Cr + Mn + Fe + Ni]) (Cressy and Bogard, 1976). For P_{21}, the equation parameters have been slightly modified from those given by Lorenzetti et al. (2003). The equation used in this work is $P_{21} = 3.84\ P'_{21}\ [18.35\ (^{22}Ne/^{21}Ne)_c - 16.65\ ]^{-1}$, where $(^{22}Ne/^{21}Ne)_c$ is the cosmogenic ^{22}Ne/^{21}Ne ratio of the sample and $P'_{21} = 1.63$ [Mg] + 0.6 [Al] + 0.32 [Si] + 0.22 [S] + 0.07 [Ca] + 0.021 [Fe+Ni] (Schultz and Freundel, 1985). The units are 10^{-10} cm^{3}STP/g/Ma for P_3 and P_{21}, and wt.% for the target element contents. More details for P_3 and P_{21} are given in electronic annex EA-4. The P_3 and P_{21} values and cosmic-ray exposure ages obtained are summarized in Table 3. The cosmic-ray exposure ages for each aubrite vary beyond experimental error (≤ 10%). If heterogeneity of the chemical composition is a reason for the variation, the ages from ^{3}He (T_3) must be less variable than those from ^{21}Ne (T_{21}) because cosmogenic ^{3}He is less sensitive to target element compositions. However, T_3 shows a large variation, and appears to be correlated with T_{21}. Therefore, variable ages probably imply pre-irradiation, complex irradiation, or inadequate correction for shielding. The evidence of being breccias (containing SW noble gases, showing neutron capture effects and including chondritic inclusions) found in many aubrites might support that idea, which is described below in greater detail.

3.5. Cosmic-ray exposure ages

The ^{81}Kr-Kr method (Eugster et al., 1967; Marti, 1967a) permits calculation of cosmic-ray

exposure ages from measured Kr isotope ratios. It is useful for meteorites with terrestrial ages << $T_{1/2}$ (^{81}Kr), i.e., for most non-Antarctic meteorites. The method eliminates uncertainty arising from determination of absolute concentrations and sample heterogeneity, giving more reliable cosmic-ray exposure ages. However, the abundances of target elements for cosmogenic Kr such as Rb, Sr and Y are low in aubrites (one or two orders of magnitude lower than those in eucrites). For this reason, detection of ^{81}Kr has been successful only for some aubrites. The measured concentrations of ^{81}Kr are approximately 10^{-14} cm^{3}STP/g (Bishopville) or lower. The ^{81}Kr-Kr age, T_{81}, was calculated combining cosmogenic radioactive ^{81}Kr and stable Kr isotopes with the formula $T_{81} = (1/\lambda_{81})\ (P_{81}/P_{83})\ (^{83}Kr/\ ^{81}Kr)_c$, where λ_{81} is the decay constant of ^{81}Kr, P_{81}/P_{83} is the production rate ratio of ^{81}Kr/^{83}Kr, and $(^{83}Kr/^{81}Kr)_c$ is the cosmogenic Kr ratio of the sample. Note that we used a decay constant of 3.25×10^{-6} years^{-1} (= a half life of 2.13×10^5 years; Eastwood et al., 1964) not the latest value of 3.03×10^{-6} years^{-1} (= 2.29×10^5 years; Baglin, 1993) to ensure consistency with previous studied referred in this paper; P_3 and P_{21} we used were calibrated using T_{81} with the former decay constant (Eugster, 1988; Lorenzetti et al., 2003 and references therein). By using the former decay constant, the cosmic-ray exposure ages presented here can be directly compared with those reported. The change of the decay constant to the latest value makes T_{81} reported here ~10% longer. The P_{81}/P_{83} was calculated as $P_{81}/P_{83} = 1.262\ (^{78}Kr/^{83}Kr)_c + 0.381$ (Marti and Lugmair, 1971). Another equation for obtaining P_{81}/P_{83} based on $(^{80}Kr/^{83}Kr)_c$ and $(^{82}Kr/^{83}Kr)_c$ (Marti, 1967a) is often not applicable to aubrites because of considerable excess $^{80, 82}$Kr from neutron captures on $^{79, 81}$Br. In Table 4, the cosmogenic Kr ratios for the samples that were determined for T_{81} are shown along with $(^{83}Kr)_c$, P_{81}/P_{83} and T_{81}. Cosmogenic Kr data for temperature steps that released significant amounts of cosmogenic Kr are given in electronic annex EA-5. We slightly revised the ages to account for a small modification of the fission correction with respect to a preliminary listing of our T_{81} by Lorenzetti et al. (2003). In addition, except for Cumberland Falls #1, we changed calculations of T_{81} using Kr data from a single temperature step to the sum of available temperature steps in a single specimen. The values of T_{81} of Norton County and Peña Blanca Spring were obtained as 113 ± 69 Ma and 63 ± 22 Ma, respectively. We present them merely to illustrate their consistency with T_3 and T_{21}. Reliable T_{81} data were obtained for four specimens of three aubrites: 52 ± 3 for Bishopville #1 (from the Kr data of 1000 and 1400°C of #1), 46 ± 12 for

Cumberland Falls #1 (1800°C), 51 ± 16 Ma for Cumberland Falls #2 (1000 and 1400°C), and 117 ± 14 Ma for Mayo Belwa #1 (1800°C). These temperature steps released the largest fractions of cosmogenic Kr (Table 4). Therefore, artificial isotope fractionation must be negligible. The cosmic-ray exposure age of 117 Ma for Mayo Belwa is the longest ^{81}Kr-Kr age reported so far.

The preferred cosmic-ray exposure age of each measured aubrite is considered. As noted above, it is sometimes difficult to determine cosmic-ray exposure ages precisely in aubrites because of their complicated cosmic-ray exposure histories and chemical heterogeneity. The obtained ages might include irradiation experienced on the parent body (2π exposure) in addition to irradiation in space immediately before falling to the Earth (4π exposure). Even so, in many cases, a large fraction of the cosmogenic nuclides might have been produced during space irradiation. The cosmic-ray exposure age, T_{exp}, is chosen from T_3, T_{21} and T_{81} based on the following criteria and priority, mostly similar to those used in Lorenzetti et al. (2003). We believe that T_{81} is more reliable than T_3 and T_{21}: (i) T_{81} is adopted as T_{exp} if T_{81} has an error smaller than 30%. However, for the case where the error is > 30% or T_{81} is not available, (ii) If $T_3 < 0.75 \times T_{21}$, then T_3 is assumed to be affected by diffusion loss of He. Consequently, the average of T_{21} is adopted as T_{exp}, and (iii) For the other cases, the average of T_3 and T_{21} is adopted as T_{exp}. The obtained ages are given in Table 3. Mayo Belwa and Norton County have long cosmic-ray exposure ages over 100 Ma, the longest ages among known cosmic-ray exposure ages of stony meteorites. We show the cosmic-ray exposure ages obtained in this work and those given in Lorenzetti et al. (2003) in Fig. 2. When data from both are available, we either adopted T_{81} as determined here (Bishopville, Cumberland Falls and Mayo Belwa) or the average age of the two studies (for the other meteorites). The figure supports the suggestion by Lorenzetti et al. (2003) that the cosmic-ray exposure ages of aubrites show a non-uniform distribution. Possible numbers of impacts that released fragments from the parent body will be discussed in Section 3.7 based on the cosmic-ray exposure age distribution and characteristic features due to surface irradiation.

3.6. Neutron capture effects

Six measured aubrites, Bishopville, Cumberland Falls, Mayo Belwa, Peña Blanca Spring,

Shallowater and ALHA 78113, show the presence of neutron-capture-produced Ar, Kr and/or Xe (Table 5). The ^{35}Cl has a large thermal neutron capture cross section, which produces ^{36}Ar (^{35}Cl (n, γ) ^{36}Cl → ^{36}Ar, the half life of ^{36}Cl is 3.01 × 10^5 years). Its contribution lowers the ^{38}Ar/^{36}Ar ratio in meteorites. The ^{38}Ar/^{36}Ar ratios of 0.0851 ± 0.0004, 0.1610 ± 0.0026, 0.1289 ± 0.0004, and 0.1647 ± 0.0009 observed in the 600°C steps of Cumberland Falls #3, Cumberland Falls #4, Shallowater and ALHA 78113, respectively, are lower than the ratios of trapped (~0.187) and cosmogenic (~1.55) Ar, and are explained by the contribution from neutron captures by Cl. All these samples also show excess $^{80, 82}$Kr produced from neutron captures by $^{79, 81}$Br. Assuming the trapped ^{38}Ar/^{36}Ar ratios (either 0.187 of Q or 0.188 of the terrestrial atmosphere) as the end member, the concentrations of neutron capture ^{36}Ar, $(^{36}Ar)_n$, are calculated as 2.3, 0.31, 0.64 and 0.14 × 10^{-9} cm^3STP/g, respectively, for the four samples. These concentrations are lower limits because the calculation assumes that (i) cosmogenic Ar was not released at the 600°C steps and (ii) neutron capture Ar was released only at 600°C. An Ar-Ar measurement of Shallowater by Bogard et al. (1995) shows that $(^{36}Ar)_n$ was released largely around 1200°C. These authors reported concentrations of $(^{36}Ar)_n$, 41 and 227 × 10^{-9} cm^3STP/g, for two samples, which are much higher than $(^{36}Ar)_n$ in this work. Because the latter concentration of 227 × 10^{-9} cm^3STP/g is similar to the measured ^{36}Ar concentration in our sample, the large differences are not attributable solely to the assumptions in evaluating $(^{36}Ar)_n$. The Cl abundances of the samples and/or neutron fluences must also be different. Neutron fluences for the four samples were calculated from $(^{36}Ar)_n$ and Cl abundances using the thermal neutron cross section of ^{35}Cl (43.6 barn; JENDL-3.3, 2002). Chlorine abundances of 164 and 416 ppm reported by Bogard et al. (1995) and Garrison et al. (2000), respectively, were adopted for Shallowater. Average Cl of 20 ppm (12, 31 and 18 ppm for Bishopville, Norton County and Peña Blanca, respectively) was adopted for the other three samples. Thermal neutron fluences were obtained to be (5.5 and 0.74), (0.19 and 0.074) and 0.34 × 10^{15} n/cm^2 for Cumberland Falls (#3 and #4), Shallowater for two different Cl values, and ALHA 78113, respectively. These neutron fluences are an order of magnitude lower than those obtained based on Sm and Gd isotopes for each aubrite, 39.9, 1.2 and 11.7 × 10^{15} n/cm^2, respectively (Hidaka et al., 1999; Hidaka et al., 2006). Moreover, the Cl abundance of 12 ppm and the thermal neutron fluence based on neutron capture Sm and Gd for Bishopville (20 × 10^{15} n/cm^2) give 5 ×

10^{-9} cm^3STP/g as $(^{36}Ar)_n$, which is compatible to the measured ^{36}Ar concentration in Bishopville. We suspect, in most cases, either that ^{36}Ar produced from ^{35}Cl was lost because of thermal metamorphism or that the Cl abundance in the measured sample is much smaller than the Cl abundances reported. If the thermal metamorphism is the reason for the deficit of $(^{36}Ar)_n$, then the heating must have been at subsolidus temperature, where neutron capture Ar was lost, but fission Xe was retained as will be shown. Alternatively Cl and U are in sites with different retentivities, leading only to loss of neutron capture Ar. For Cumberland Falls, only specimens #3 and #4 show remarkable $(^{36}Ar)_n$. Furthermore, #3 and #4 have an order of magnitude higher $(^{80}Kr)_n$, $(^{82}Kr)_n$ and $(^{128}Xe)_n$ than #1 and #2. As the correlation of $(^{128}Xe)_n$ with $(^{129}Xe)_{rad}$ in Cumberland Falls indicates, higher concentrations of these neutron-capture-produced noble gases are attributable to higher abundances of halogens.

^{80}Kr and ^{82}Kr are produced from neutron captures on ^{79}Br and ^{81}Br, respectively, with large epithermal neutron capture cross sections. In the plot $^{80}Kr/^{84}Kr$ vs. $^{82}Kr/^{84}Kr$ (Fig. 3), several temperature steps of Cumberland Falls #1, #3 and #4, Shallowater and ALHA 78113 plot towards composition of neutron capture Kr, indicating that most of the excess ^{80}Kr and ^{82}Kr for these steps consists of neutron capture products. The Kr data of other aubrites plot near the line towards cosmogenic Kr (e.g., some steps of Bishopville, Mt. Egerton, Norton County and Peña Blanca Spring), near the composition of trapped Kr (e.g. Norton County), or between these components. After subtracting trapped Kr, the $^{80}Kr/^{83}Kr$ and $^{82}Kr/^{83}Kr$ ratios in temperature steps where cosmogenic Kr is dominant (e.g., 0.559 ± 0.030 and 0.763 ± 0.040, respectively, in 1000°C of Bishopville) agree well with the assumed cosmogenic Kr spectra, supporting that the assumed cosmogenic values are reasonable. After subtracting trapped and cosmogenic Kr, neutron capture Kr was well discernible in Bishopville, Cumberland Falls, Mayo Belwa, Peña Blanca Spring, Shallowater, and ALHA 78113. The concentrations of $(^{80}Kr)_n$ and ratios of $(^{80}Kr/^{82}Kr)_n$ are summarized in Table 5. The respective values of $(^{80}Kr)_n$ for the six aubrites were calculated as 0.8, (0.7–199), 4.9, (0.3–0.4), 15 and 1.2×10^{-12} cm^3STP/g. Up to 95% of the total excess ^{80}Kr is the neutron capture Kr in Cumberland Falls #3 and #4 and Shallowater. The observed $(^{80}Kr/^{82}Kr)_n$ is 2.70 ± 0.09, 2.74 ± 0.19, 2.71 ± 0.78 for reliable temperature steps of these samples (Table 5), respectively, which is consistent with the theoretical production ratio of 2.62 at the energy range of 30–300 eV (Marti et al.,

1966) and the observed ratios of 2.66 and 2.69 in the L3 chondrite Yamato (Y) -74191 (Nagao and Takaoka, 1979; Takaoka and Nagao, 1980). The $(^{80}Kr/^{82}Kr)_n$ of 1.46 ± 0.34 for Bishopville is close to the production ratio of 1.63 in the higher neutron energy range of 10–100 keV (Marti et al., 1966). However, because the neutron capture cross section in this energy range is 50–100 times lower than that in the 30–300 eV range, it seems unlikely that this is due to neutron capture at high energy. Alternatively, cosmogenic Kr composition in the 600°C step of Bishopville may be different from what we assumed. Because only 4% of the total cosmogenic ^{83}Kr was released at 600°C, cosmogenic ratios might differ from those of bulk samples. Because the fraction of cosmogenic Kr is large, the $(^{80}Kr/^{82}Kr)_n$ evaluation is sensitive to the assumed cosmogenic ratios.

^{128}Xe produced from neutron capture on ^{127}I is also found in three aubrites. We first investigate cosmogenic Xe compositions using three-isotope plots to evaluate $(^{128}Xe)_n$ more accurately. Figure 4 shows the diagram $^{124}Xe/^{130}Xe$ vs. $^{126}Xe/^{130}Xe$. These Xe isotopes generally comprise mixtures of cosmogenic and trapped components. Several data, 1000 and 1400°C of Bishopville, 1000°C of Cumberland Falls #2, 1800°C of Cumberland Falls #4, 1800°C of Mayo Belwa and 1800°C of Peña Blanca Spring #1, #3, #4 and #5, plot outside the cosmogenic ratios inferred for aubritic chemistry (calculated as mixture of LREE and Ba spallation Xe assuming LREE and Ba abundances of the average for aubrites; Busemann et al., 2000) and plot near the direction of cosmogenic Xe for Ba target (Hohenberg et al., 1981). Three-isotope plots using other Xe isotopes, like $^{131}Xe/^{130}Xe$ vs. $^{126}Xe/^{130}Xe$ and $^{132}Xe/^{130}Xe$ vs. $^{126}Xe/^{130}Xe$ (electronic annex EA-6), show a similar behaviour. Although ^{131}Xe and ^{132}Xe are enhanced by fission Xe in some samples, the ratios after fission Xe correction fall near cosmogenic Xe ratios for aubritic chemistry. Heavy shielding cannot explain the data plotting towards Ba spallation. Heavy shielding lowers $^{124}Xe/^{130}Xe$ and simultaneously increases $^{131}Xe/^{130}Xe$ substatially, but the data towards Ba spallation show low $^{124}Xe/^{130}Xe$ and $^{131}Xe/^{130}Xe$ ratios. Therefore, we adopted spallation spectra for Ba target chemistry for the temperature steps listed above and those for aubritic chemistry for the others in decomposition of Xe. After correction of cosmogenic Xe, Cumberland Falls, Mayo Belwa and Shallowater indicate excess ^{128}Xe, which is attributable to ^{128}Xe from neutron capture on ^{127}I. The absolute concentrations of $(^{128}Xe)_n$ vary by about

two orders among the measured specimens of Cumberland Falls.

Many aubrites have radiogenic ^{129}Xe, as presented in Table 6. Figure 5 shows ^{128}Xe/^{130}Xe vs. ^{129}Xe/^{130}Xe after cosmogenic correction. Different pieces of Cumberland Falls have a constant $(^{128}Xe)_n/(^{129}Xe)_{rad}$ ratio despite large variations in $(^{128}Xe)_n$ and $(^{129}Xe)_{rad}$ concentrations (Tables 5 and 6). Therefore, the variable concentrations are not due to differences in neutron fluence nor in retention time for $(^{129}Xe)_{rad}$, but rather due to heterogeneous iodine distribution. The $(^{128}Xe)_n/(^{129}Xe)_{rad}$ ratios are, however, different among the three measured aubrites: Mayo Belwa (0.045), Cumberland Falls (0.015) and Shallowater (0.001). The difference in the ratios must be the results of the difference in neutron fluences, retention ages for radiogenic ^{129}Xe or both.

3.7. Exposure histories of aubrites

Neutron capture effects on other nuclides were reported for aubrites. Hidaka et al. (1999, 2003 and 2006) determined thermal neutron fluences for ten aubrites based on shifts of neutron capture Sm and Gd isotopes. Bishopville, Cumberland Falls and Pesyanoe show the highest neutron fluences among aubrites. These fluences are higher than those inferred from their cosmic-ray exposure ages. Neutron fluences are shown schematically together with comic-ray exposure ages in Fig. 2. Welten et al. (2002 and 2004) measured the radionuclide ^{41}Ca (half life = 1.03×10^5 years) produced from neutron capture on ^{40}Ca in aubrites. The ^{41}Ca is saturated after an exposure of $\sim 5 \times 10^5$ years, which can be used to estimation the neutron flux during a recent exposure. Total fluences were calculated from fluxes and cosmic-ray exposure ages. Because the thermal neutron fluences based on Sm and Gd are higher than those based on ^{41}Ca for the above three aubrites (and slightly higher in Mayo Belwa and Norton County), Welten et al. (2004) concluded that parts of neutron capture Sm and Gd were produced early, likely on the parent body. Assuming that the aubrites were exposed at a depth of 150 g/cm^2 on the parent body (at the maximum thermal neutron flux), minimum exposure ages were obtained as 105 Ma for Cumberland Falls (the largest difference in fluences between Sm-Gd and ^{41}Ca), 70 Ma for Pesyanoe, 57 Ma for Bishopville, 45 Ma for Mayo Belwa and 24 Ma for Norton County (the smallest but significant difference), respectively (Welten

et al., 2004). On the other hand, no differences in neutron fluences were found in Mt. Egerton and Peña Blanca Spring, that is, the total fluences based on Sm and Gd isotope shifts can be explained by production during irradiation in space (Welten et al., 2004). Neutron fluence of LAP 02233 determined based on Sm isotope shift is 6.9×10^{15} n/cm^2 (experimentation and the isotope data are given in electronic annex EA-7), which is about twice that of Peña Blanca Spring (3×10^{15} n/cm^2, T_{exp} = 75 Ma) and about half that of Norton County (15×10^{15} n/cm^2, T_{exp} = 121 Ma). Considering the age of LAP 02233 (78 Ma), it might contain a small contribution of neutron capture Sm that has been produced on the parent body.

Neutron-capture-produced noble gases were not observed in Mt. Egerton, Norton County and LAP 02233, and only a small contribution of $(^{80}Kr)_n$ was detected for Peña Blanca Spring. Results for noble gases and Sm isotopes indicate that these aubrites were unaffected (or less affected) by secondary neutrons and were possibly buried in deeper parts on the parent body than other aubrites. In contrast, Bishopville and Cumberland Falls, which showed large excess neutron fluences attributable to effects on the parent body, exhibit neutron-capture-produced noble gases. These two aubrites are likely to have resided in shallower parts of their parent body and to have been influenced by neutron capture effects. Mayo Belwa and ALHA 78113 were probably located at slightly larger depths than Bishopville and Cumberland Falls. An exception is Shallowater, which shows neutron capture ^{36}Ar, ^{80,82}Kr and ^{128}Xe, but no excess of neutron capture Sm and Gd. Because Shallowater has a higher Cl content than other aubrites, abundances of other halogens, Br and I, might also be high, leading abundant neutron-capture-produced noble gases. Apparently, only aubrites with evidence of exposure at the surfaces of the parent body (except Shallowater) tend to have neutron-capture-produced noble gases. Therefore, an irradiation process other than recent irradiation in space may be the major reason for the remarkable amounts of neutron-capture-produced noble gases in aubrites.

Figure 2 summarizes the cosmic-ray exposure ages and sample characteristics. Among 22 aubrites studied for cosmic-ray exposure ages so far, most are breccias, seven aubrites contain SW noble gases, six aubrites show neutron-capture-produced noble gas nuclides (four of them also show excess neutron captures on Sm attributable to production in the parent body), three aubrites indicate incorporation of chondritic noble gases supplied from chondritic inclusions, and one aubrite (Shallowater) has chondritic

primordial noble gases. Based on these features and the cosmic-ray exposure ages, possible numbers of break-up events that released aubrite fragments into space from the parent body(ies) are considered. In the present discussion, Mt. Egerton and Shallowater are not counted, because both are anomalous in some respects compared to most other aubrites. Shallowater probably came from a different parent body. Mt. Egerton, however, might originate from the mantle-core boundary in the common parent body to most aubrites. If we assumed that some differences in cosmogenic nuclide concentrations are due to pre-exposure on the parent body, the distribution shown in Fig. 2 can be classified into four groups and ALH aubrites are considered to be fragments of a single fall. The minimum number of break-up events seems to be four. On the other hand, if we assume that cosmogenic nuclide concentrations reflect entirely 4π cosmic-ray exposure ages, up to nine break-up events could have occurred. An important question is whether two aubrites, Bishopville and Cumberland Falls, are related to the aubrite group containing SW noble gases. A salient possibility is that all these aubrites have the same 4π cosmic-ray exposure ages but largely different 2π parent body exposure ages.

3.8. Trapped noble gases

The measured aubrites contain trapped Ar, Kr and Xe including probably adsorbed terrestrial atmosphere. A purpose of this section is to identify the compositions and origin of the trapped components. The concentrations of bulk $(^{36}Ar)_t$, $(^{84}Kr)_t$ and $(^{132}Xe)_t$, and the ratios of $(^{36}Ar/^{132}Xe)_t$ and $(^{84}Kr/^{132}Xe)_t$ (sum of all crushing and heating steps) are shown in Table 7, and the plot $(^{36}Ar/^{132}Xe)_t$ vs. $(^{84}Kr/^{132}Xe)_t$ are displayed in Fig. 6(a). Also shown in the figure are typical chondritic compositions ("Q") and an Ar-rich component represented by the enstatite chondrite South Oman. Note that the Ar-rich gas might not be an inherent component by itself (Busemann et al., 2003), but this composition is widely observed particularly in enstatite chondrites. The dotted lines indicate mass fractionation trends and/or mixtures between e.g., the Ar-rich and Q gases. Here the area between Q and Ar-rich gases is called chondrite data trend (because many chondrite data plot on the area). On this plot, data for Cumberland Falls and Shallowater fall on the chondrite data trend. In Fig. 6(b) crushing and heating data of four aubrites showing signatures of

chondritic Ar, Kr and Xe are plotted. Although bulk data of Peña Blanca Spring and ALHA 78113 plot on the terrestrial atmospheric mass fractionation trend, several heating steps are plotted near the chondrite data trend. Shallowater, an anomalous aubrite, has the highest concentrations of Ar, Kr and Xe among aubrites except for Pesyanoe that contains a large amount of SW noble gases (Kim and Marti, 1992; Mathew and Marti, 2003). The respective concentrations of trapped ^{36}Ar, ^{84}Kr and ^{132}Xe in Shallowater are 218×10^{-9}, 937×10^{-12} and 283×10^{-12} cm^{3}STP/g, which are similar to those reported by Busemann and Eugster (2002), 241×10^{-9}, 1001×10^{-12} and 551×10^{-12} cm^{3}STP/g. These trapped noble gas concentrations are comparable to those found in some carbonaceous chondrite clans (e.g. CK chondrites; Scherer and Schultz, 2000) and ordinary chondrites of petrographic type 4-5 (e.g., Marti, 1967b; Zähringer, 1968). The Ar/Kr/Xe elemental composition of Shallowater is enriched in lighter noble gases compared to these chondrites and falls between Q and the Ar-rich composition. The isotopic composition of Xe for 1800°C of Shallowater is shown as permil deviation relative to the terrestrial atmospheric Xe (δ^mXe) in Fig. 7(a). The δ^mXe of Shallowater agrees with that of Q-Xe, except for ^{129}Xe enhanced by radiogenic ^{129}Xe. Isotopic compositions of Kr are consistent with Q-Kr and also the terrestrial atmospheric Kr within error. The indigenous noble gas signature in Shallowater has not been greatly altered.

The concentrations of trapped noble gases in Cumberland Falls, Peña Blanca Spring and ALHA 78113 are much lower than those in Shallowater. Ar, Kr and Xe in these meteorites are affected by cosmogenic gases. Only Xe in the 1800°C step of Cumberland Falls #3 shows an isotopic composition that is similar to Q-Xe (Fig. 7(b)). The trapped Kr and Xe concentrations in Cumberland Falls #3 are 10 and 30 times higher than those in #1. Because heterogeneous incorporation of chondritic inclusions has been inferred from petrological and oxygen isotopic studies, abundances of trapped chondritic noble gases are indeed expected to be variable. It is also noteworthy that the Ar/Kr/Xe elemental compositions are not constant among the measured specimens. Compositions of #1, #2 and #4 plot near the Ar-rich composition, whereas those of #3 and those measured in Busemann and Eugster (2002) plot close to Q. The variable gas concentrations and Ar/Kr/Xe compositions might be explained by admixture of chondritic materials with variable Ar/Kr/Xe compositions to the aubrite parent body. Alternatively, the Ar/Kr/Xe composition of chondrite materials was constant, but it was changed by subsequent alteration leading to partial loss of

trapped noble gases. The presence of chondritic inclusions was also reported for ALHA 78113 (Lipschutz et al., 1988). The 1800°C step of ALHA 78113 released Ar, Kr and Xe with an elemental composition close to Q (Fig. 6 (b)). Peña Blanca Spring #2 and #5 also released small amounts of trapped Ar, Kr and Xe with a composition near South Oman. Approximately half of the measured heavy noble gases are assigned chondritic and the rest as terrestrial atmospheric contamination in Peña Blanca Spring #2 and ALHA 78113. Because the noble gas concentrations in chondritic inclusions must be higher than those in aubrite hosts, a small proportion of inclusions might be sufficient to change the noble gas composition of a bulk sample. Although chondritic inclusions in Peña Blanca Spring have not been reported, we expect that microscopic chondritic fragments are heterogeneously distributed.

3.9. Fission Xe from ^{244}Pu

Figure 8 shows the plot of ^{134}Xe/^{130}Xe vs. ^{136}Xe/^{130}Xe after cosmogenic correction. Cumberland Falls, Mayo Belwa and Peña Blanca Spring (only #2) clearly indicate the addition of fission Xe. Both ALHA 78113 and LAP 02233 also show a small excess attributable to fission Xe. The Xe in the other aubrites is scattered around the terrestrial atmospheric Xe or Q-Xe. The Xe in 1800°C of Peña Blanca Spring #1 and #5 appeared to be near solar Xe, however, this might merely reflect the contribution of cosmogenic Xe from Cs. Aubrites have high abundances of Cs relative to the other cosmogenic Xe target elements, LREE and Ba. In particular, Peña Blanca Spring shows higher Cs contents (an average of 368 ppm from five data compiled in Koblitz J., 2005, MetBase 7.1) than other aubrites (65 ppm from 21 data of 12 aubrites), which probably enhances cosmogenic ^{130}Xe, ^{131}Xe and ^{132}Xe from ^{133}Cs. Therefore, a shift to solar Xe may not be an unambiguous signature for trapped Xe. As revealed by the figure, the majority of fission Xe is likely to arise from spontaneous fission of ^{244}Pu rather than from ^{238}U or neutron-induced fission of ^{235}U. The concentrations of $(^{136}Xe)_f$ in Cumberland Falls only vary by factor of three (Table 6), much less than $(^{129}Xe)_{rad}$ in this aubrite, and $(^{136}Xe)_f$ is not correlated with $(^{129}Xe)_{rad}$. Behaviors of the parent elements, Pu and I, must not have been coherent during differentiation. The isotopic spectra of fission Xe for the temperature steps that released marked excess of Xe are shown in Table 6. ^{134}Xe/^{136}Xe

agrees well with the value for ^{244}Pu fission, and ^{131}Xe and ^{132}Xe are also close to ^{244}Pu fission Xe than expectation for ^{238}U and ^{235}U fission. However, we try to evaluate a possible ^{238}U contribution based on reported U contents. Bulk U contents have been reported for six of these nine measured aubrites: 4.40 ppb for Bishopville (average of three data by Morgan and Lovering, 1973; Wolf et al., 1983; Ebihara et al., private com.), 22.5 ppb for Cumberland Falls (Ebihara et al., private com.), 5.76 ppb for Mayo Belwa (Ebihara et al., private com.), < 10 ppb for metal phase of Mt. Egerton (Wolf et al., 1983), < 15 ppb for silicate phase of Mt. Egerton (Wolf et al., 1983), 4.62 ppb for Norton County (average of three data by Morgan and Lovering, 1973; Wolf et al., 1983; Ebihara et al., private com.), and 8.6 ppb for Peña Blanca Spring (Wolf et al., 1983). From these values, we obtained concentrations of ^{238}U-derived fission ^{136}Xe, $(^{136}Xe)_U$, to be 0.015, 0.078, 0.020, 0.016 and 0.030 × 10^{-12} cm^3STP/g for Bishopville, Cumberland Falls, Mayo Belwa, Norton County and Peña Blanca Spring, respectively, and 0.016 × 10^{-12} cm^3STP/g for an average U content of aubrites (4.5 ppb; Mason, 1979). Fractions of ^{136}Xe from ^{238}U to the total fission, $(^{136}Xe)_U/(^{136}Xe)_f$, are obtained to be 8-24, 6, 7, 11 and 10% for Cumberland Falls, Mayo Belwa, Peña Blanca Spring, ALHA 78113 and LAP 02233, respectively, adopting U contents of each aubrite for the former three and the average value for the latter two aubrites. These figures indicate that 80-90% of $(^{136}Xe)_f$ is indeed ^{244}Pu derived fission, in agreement with the observed Xe spectra. The corresponding ^{244}Pu abundances are calculated to be from 0.019 to 0.16 ppb; (0.04–0.16), 0.05, 0.06, 0.02 and 0.02 ppb, respectively, for the five aubrites, yielding ^{244}Pu/U ratios of 0.002–0.007, 0.009, 0.007, 0.004 and 0.005, respectively. These ^{244}Pu/U ratios, although varying by a factor of three within Cumberland Falls, are within values reported for other achondrites such as eucrites (e.g. 0.003–0.005 by Podosek, 1972; Miura et al., 1993) and chondrites (e.g. 0.004–0.007 by Podosek and Swindle, 1988; Hagee et al., 1990). This fact implies that (i) aubrites have approximately the same ^{244}Pu/U ratios as other meteorites, (ii) retention of Xe was started early when ^{244}Pu was still existent in the parent body, and (iii) extensive thermal heating that reset Pu-Xe system did not occur after Xe retention started at ~4.5 Ga ago. Only a few chronologic data have been reported for aubrites; the most precise age is 4.5633 ± 0.0004 Ga for Shallowater (the age converted based on relation between I-Xe and P-Pb ages; Gilmour et al., 2006), the reported I-Xe ages are 20.8 ± 9.5, -0.6, 3.6 ± 0.7 and -0.5 ± 0.6 Ma (+ and - indicate later and earlier than the L4 chondrite

Bjurbölel, respectively) for Bishopville, two data of Shallowater and Peña Blanca Spring, respectively (Hohenberg, 1967; Podosek, 1970; Whitby et al., 2002), and the reported Rb-Sr age is 3.7 ± 0.2 Ga for Bishopville (Compston et al., 1965). Results from ^{244}Pu-Xe and I-Xe are mutually consistent for the common sample of Peña Blanca Spring. The non-detection of ^{244}Pu fission Xe supports the late I-Xe age for Bishopville.

4. SUMMARY

(1) Using the ^{81}Kr-Kr method, cosmic-ray exposure ages were obtained to be 52 ± 3, 49 ± 10, 117 ± 14 Ma, respectively, for Bishopville, Cumberland Falls and Mayo Belwa. For the other measured aubrites, the following values were calculated as the most reliable cosmic-ray exposure ages: 28 ± 4 Ma (Mt. Egerton), 121 ± 16 Ma (Norton County), 75 ± 11 Ma (Peña Blanca Spring), 28 ± 4 Ma (Shallowater), 23 ± 4 Ma (ALHA 78113), and 78 ± 12 Ma (LAP 02233). The ages of 117 Ma for Mayo Belwa and 121 Ma for Norton County are the longest cosmic-ray exposure ages among stony meteorites. Peña Blanca Spring and LAP 02233 show similar exposure ages of 75 and 78 Ma, which are also long. Distribution of cosmic-ray exposure ages for aubrites seems to be non-uniform, and between four and nine break-up events occurred on the parent body (if the anomalous aubrites Mt. Egerton and Shallowater are not considered).

(2) Thermal or epithermal neutron-capture-produced noble gases, ^{36}Ar, ^{80}Kr, ^{82}Kr and/or ^{128}Xe, are found in Bishopville, Cumberland Falls, Mayo Belwa, Peña Blanca Spring, Shallowater and ALHA 78113. Because these aubrites, aside from Peña Blanca Spring and Shallowater, show excess neutron fluences that were considered to have been produced on the parent body(ies) (Hidaka et al., 1999, 2003 and 2006; Welten et al., 2004), neutron capture noble gases were also likely produced on their parent body(ies). The concentrations of $(^{128}Xe)_n$ vary by two orders of magnitude among the four measured specimens of Cumberland Falls, and correlate with the concentrations of radiogenic ^{129}Xe, $(^{129}Xe)_{rad}$. This fact implies that both neutron fluences and radiogenic ^{129}Xe retention ages are similar among these specimens; the variable concentrations of $(^{128}Xe)_n$ and $(^{129}Xe)_{rad}$ are attributable to variable abundances of the target element iodine. The ratios of $(^{128}Xe)_n/(^{129}Xe)_{rad}$ obtained in this study are in the following order: Mayo

Belwa (0.045) > Cumberland Falls (0.015) > Shallowater (0.001). The difference in the ratios is ascribed to different neutron fluences and/or different radiogenic ^{129}Xe retention ages.

(3) Fission derived Xe is found in Cumberland Falls, Mayo Belwa, Peña Blanca Spring, ALHA 78113 and LAP 02233. Most fission Xe is thought to originate from ^{244}Pu-derived fission based on isotopic spectra, and about 10–20% fission Xe (at ^{136}Xe) is calculated as ^{238}U-derived fission based on reported U contents. The concentrations of ^{136}Xe from ^{244}Pu are calculated as 1.2-10 × 10^{-13} cm^3STP/g, corresponding to 0.02–0.16 ppb of ^{244}Pu. These ^{244}Pu abundances and reported U contents give ^{244}Pu/U ratios of 0.002–0.009, which are similar to those reported for chondrites and achondrites (e.g. 0.003–0.007), suggesting that extensive thermal heating that reset Pu-Xe system did not occur after Xe retention began ~4.5 Ga ago. The amounts of $(^{136}Xe)_{Pu}$ and $(^{129}Xe)_{rad}$ are not mutually correlated within a single aubrite. For that reason, behavior of Pu and I must have been different during differentiation.

(4) Bishopville, Mayo Belwa, Mt. Egerton, Norton County and LAP 02233 show only terrestrial atmospheric Ar, Kr and Xe as trapped component, whereas Cumberland Falls, Peña Blanca Spring, Shallowater and ALHA 78113 show additionally chondritic noble gases. Shallowater, an anomalous aubrite, contains abundant chondritic Ar, Kr and Xe, as reported previously (Busemann and Eugster, 2002), which is considered to be primordial in origin due to the unbrecciated nature of the meteorite. The concentrations of chondritic noble gases in the other three aubrites are low. Because Cumberland Falls and ALHA 7811 contain chondritic inclusions (Neal and Lipschutz, 1981; Lipschutz et al., 1988), they probably contain chondritic noble gases. We expect that Peña Blanca Spring also includes chondrite fragments, possibly microscopic and heterogeneously distributed, although this has not been observed directly so far. Only one of three analyses for Cumberland Falls indicates a signature of chondritic (LL or L like) oxygen isotopic compositions. According to the trapped noble gas concentrations and oxygen isotope compositions, proportions of chondrite materials are small in Peña Blanca Spring and ALHA 78113.

(5) Many aubrites show one or several regolith characteristics (this work; Lorenzetti et al., 2003 and references therein): brecciated nature, presence of implanted SW, records of neutron capture effects, and preservation of chondritic fragments. Results of the present study collaborate the idea that many impacts

have occurred on the aubrite parent body(ies) and that aubrites originated from their surface regoliths which had suffered a complex history.

Acknowledgements – We thank the National Museum of Natural History, Smithsonian Institution, U.S.A. for providing the Bishopville, Cumberland Falls, Norton County, Peña Blanca Spring and Shallowater, and Antarctic Meteorite Working Group for ALHA 78113 and LAP 02233. We are grateful to Prof. Nagao for allowing the use of the noble gas mass spectrometer and many helpful discussions. Dr. Okazaki is acknowledged for supporting crushing measurements, and Ms. Nogi is appreciated for technical assistance in oxygen isotopic analyses. We are indebted to Prof. Marti, Dr. Whitby, Dr. Nakamura, Prof. Wieler and an anonymous reviewer for constructive reviews, which resulted in substantial improvements of the manuscript. This work was supported by Grant-in-Aid No. 15540464 to Y. N. M. and No. 13440167 to H.H. from the Japan Society for the Promotion of Science.

REFERENCES

Alexander J. E. C., Lewis R. S., Reynolds J. H., and Michel M. (1971) Plutonium-244: confirmation as an extinct radioactivity. *Science* **172**, 837-840.

Baglin C. M. (1993) Nuclear data sheets update for A=81. *Nuclear Data Sheets* **69**, 267-373.

Bogard D. D., Horz F., and Johnson P. (1989) Shock-implanted noble gases II: Additional experimental studies and recognition in naturally shocked terrestrial materials. *Meteoritics* **24**, 113-123.

Bogard D. D., Nyquist L. E., Bansal B. M., Garrison D. H., Wiesmann H., Herzog G. F., Albrecht A. A., Vogt S., and Klein J. (1995) Neutron-capture ^{36}Cl, ^{41}Ca, ^{36}Ar, and ^{150}Sm in large chondrites: Evidence for high fluences of thermalized neutrons. *J. Geophys. Res.* **100**, 9401-9416.

Busemann H. and Eugster O. (2002) The trapped noble gas component in achondrites. *Meteorit. Planet. Sci.* **37**, 1865-1891.

Busemann H., Baur H., and Wieler R. (2000) Primordial noble gases in "phase Q" in carbonaceous and ordinary chondrites studied by closed-system stepped etching. *Meteorit. Planet. Sci.* **35**, 949-973.

Busemann H., Eugster O., Baur H., and Wieler R. (2003) The ingredients of the “subsolar” noble gas component. *Lunar Planet. Sci.* **XXXIV**, Lunar Planet. Inst., Houston. #1674 (abstr.).

Clayton R. N. (1993) Oxygen isotopes in meteorites. *Ann. Rev. Earth Planet. Sci.* **21**, 115-149.

Clayton R. N. (2003) Oxygen isotopes in meteorites. In *Meteorites, comets, and planets* (ed. A. M. Davis), Treatise on Geochemistry Vol. 1. Elsevier, Amsterdam. pp. 129-142.

Clayton R. N. and Mayeda T. K. (1996) Oxygen isotope studies of achondrites. *Geochim. Cosmochim. Acta* **69**, 1999-2017.

Clayton R. N., Mayeda T. K., and Rubin A. E. (1984) Oxygen isotopic compositions of enstatite chondrites and aubrites. *Proc. 15th Lunar Planet. Sci. Conf., J. Geophys. Res.* **89**, C245-C249.

Compston, W., Lovering J. F., and Vernon M. J. (1965) The rubidium-strontium age of the Bishopville aubrite and its component enstatite and feldspar. *Geochim. Cosmochim. Acta* **29**,

1085-1099.

Crabb J. and Anders E. (1981) Noble gases in E-chondrites. *Geochim. Cosmochim. Acta* **45**, 2443-2464.

Cressy P. J. and Bogard D. D. (1976) On the calculation of cosmic-ray exposure ages of stony meteorites. *Geochim. Cosmochim. Acta* **40**, 749-762.

Eastwood T. A., Brown F., and Crocker I. H. (1964) A krypton-81 half-life determination using a mass separator. *Nuclear Physics* **58**, 328-336.

Eikenberg J., Signer P., and Wieler R. (1993) U-Xe, U-Kr, and U-Pb systematics for dating uranium minerals and investigations of the production of nucleogenic neon and argon. *Geochim. Cosmochim. Acta* **57**, 1053-1069.

Eugster O. (1988) Cosmic-ray production rates for ^{3}He, ^{21}Ne, ^{38}Ar, ^{83}Kr and ^{126}Xe in chondrites based on ^{81}Kr-Kr exposure ages. *Geochim. Cosmochim. Acta* **52**, 1649-1662.

Eugster O. and Michel T. (1995) Common asteroid break-up events of eucrites, diogenites, and howardites and cosmic- ray production rates for noble gases in achondrites. *Geochim. Cosmochim. Acta* **59**, 177-199.

Eugster O., Eberhardt P., and Geiss J. (1967) ^{81}Kr in meteorites and ^{81}Kr radiation ages. *Earth Planet. Sci. Lett.* **2**, 77-82.

Eugster O., Eberhardt P., and Geiss J. (1969) Isotopic analyses of krypton and xenon in fourteen stone meteorites. *J. Geophys. Res.* **74**, 3874-3896.

Garrison D., Hamlin S., and Bogard D. (2000). Chlorine abundances in meteorites. *Meteorit. Planet. Sci.* **35**, 419-429.

Gilmour J. D., Pravdivtseva O. V., Busfield A., and Hohenberg C. M. (2006) The I-Xe chronometer and the early solar system. *Meteorit. Planet. Sci.* **41**, 19-31.

Gonfiantini R., Stichler W., and Rozanski K. (1995) Reference and intercomparison materials for stable isotopes of light elements. *IAEA-TECDOC-825*, 13.

Hagee B., Bernatowicz T. J., Podosek F. A., Johnson M. L., Burnett D. S., and Tatsumoto M. (1990) Actinide abundances in ordinary chondrites. *Geochim. Cosmochim. Acta* **54**, 2847-2858.

Hidaka H., Ebihara M., and Yoneda S. (1999) High fluences of neutrons determined from Sm and Gd isotopic compositions in aubrites. *Earth Planet. Sci. Lett.* **173**, 41-51.

Hidaka H., Yoneda S., and Marti K. (2003) Regolith history of the aubrite parent body. *Meteorit. Planet. Sci.* **38**, A60 (abstr.).

Hidaka H., Yoneda S., and Marti K. (2006) Regolith history of the aubritic meteorite parent body revealed by neutron capture effects on Sm and Gd isotopes. *Geochim. Cosmochim. Acta* **70**, 3449-3456.

Hohenberg C. M. (1967) I-Xe dating of the Shallowater achondrite. *Earth Planet. Sci. Lett.* **3**, 357-362.

Hohenberg C. M., Hudson B., Kennedy B. M., and Podosek F. A. (1981) Xe spallation systematics in Angra dos Reis. *Geochim. Cosmochim. Acta* **45**, 1909-1915.

Japanese Evaluated Nuclear Data Library (JENDL) 3.3. (2002) Nuclear Data Center at Japan Atomic Energy Research Institute, Ibaraki, Japan.

Keil K. (1989) Enstatite meteorites and their parent bodies. *Meteoritics* **23**, 195-208.

Keil K., Ntaflos T., Taylor G. J., Brearley A. J., Newsom H. E., and Romig A. D. Jr. (1989) The Shallowater aubrites: Evidence for origin by planetesimal impact. *Geochim. Cosmochim. Acta* **53**, 3291-3307.

Kim J. S. and Marti K. (1992) Solar-type xenon: Isotopic abundances in Pesyanoe. *Proc. Lunar Planet. Sci. Conf.* **22**, 145-151.

Kusakabe M., Maruyama S., Nakamura T., and Yada T. (2004) CO_2 laser-BrF_5 fluorination technique for analysis of oxygen three isotopes of rocks and minerals. *J. Mass Spectromet. Soc. Japan* **52**, 205-212.

Lipschutz M. E., Verkouteren R. M., Sears D. W. G., Hasan F. A., Prinz M., Weisberg M. K., Nehru C. E., Delaney J., Grossman L., and Boily M. (1988) Cumberland Falls chondritic inclusions - III. Consortium study of relationship to inclusions in Allan Hills 78113 aubrite. *Geochim. Cosmochim. Acta* **52**, 1835-1848.

Lorenzetti S., Eugster O., Busemann H., Marti K., Burbine T. H., and McCoy T. (2003) History and

origin of aubrites. *Geochim. Cosmochim. Acta* **67**, 557-571.

Marti K. (1967a) Mass-spectrometric detection of cosmic-ray-produced ^{81}Kr in meteorites and the possibility of Kr-Kr dating. *Phys. Rev. Lett.* **18**, 264-266.

Marti K. (1967b) Trapped xenon and the classification of chondrites. *Earth Planet. Sci. Lett.* **2**, 193-196.

Marti K. and Lugmair G. W. (1971) Kr^{81}-Kr and K-Ar^{40} ages, cosmic-ray spallation products, and neutron effects in lunar samples from Oceanus Procellarum. *Proc. Lunar Sci. Conf.* **2**, 1591-1605.

Marti K., Eberhardt P., and Geiss J. (1966) Spallation, fission, neutron capture anomalies in meteoritic krypton and xenon. *Z. Naturforschung* **21a**, 398-413.

Mason B. (1979) Cosmochemistry., Part 1. Meteorites. U.S. Geological Survey Professional Paper, 440-B-1, 132p., Washington, D.C.

Mathew K. J. and Marti K. (2003) Solar wind and other gases in the regoliths of the Pesyanoe parent object and the moon. *Meteorit. Planet. Sci.* **38**, 627-643.

Miura Y., Nagao K., and Fujitani T. (1993) ^{81}Kr terrestrial ages and grouping of Yamato eucrites based on noble gas and chemical compositions. *Geochim. Cosmochim. Acta* **57**, 1857-1866.

Miura Y. N., Nagao K., Sugiura N., Sagawa H., and Matsubara K. (1995) Orthopyroxenite ALH84001 and shergottite ALH77005: Additional evidence for a martian origin from noble gases. *Geochim. Cosmochim. Acta* **59**, 2105-2113.

Miura Y. N., Nagao K., Sugiura N., Fujitani T., and Warren P. H. (1998) Noble gases, ^{81}Kr-Kr exposure ages and ^{244}Pu-Xe ages of six eucrites, Béréba, Binda, Camel Donga, Juvinas, Millbillillie, and Stannern. *Geochim. Cosmochim. Acta* **62**, 2369-2387.

Morgan J. W. and Lovering J. F. (1973) Uranium and thorium in achondrites. *Geochim. Cosmochim. Acta* **37**, 1697-1707.

Nagao K. and Takaoka N. (1979) Rare Gas Studies of Antarctic Meteorites. *Mem. Natl. Inst. Polar Res., Spec. Issue* **12**. Natl. Inst. Polar Res., Tokyo. 207-222.,

Nagao K., Okazaki R., Sawada S., and Nakamura N. (1999) Noble gases and K-Ar ages of five

Rumuruti chondrites Yamato (Y)-75302, Y-791827, Y-793575, Y-82002, and Asuka-881988. *Antarct. Meteorit. Res.* **12**, 81-93.

Neal C. and Lipschutz M. E. (1981) Cumberland Falls chondritic inclusions: Mineralogy/petrology of a forsterite chondrite suite. *Geochim. Cosmochim. Acta* **45**, 2091-2107.

Newton J., Franchi I. A., and Pillinger C. T. (2000) The oxygen isotopic record in enstatite meteorites. *Meteorit. Planet. Sci.* **35**, 689-698.

Niedermann S. and Eugster O. (1992) Noble gases in lunar anorthositic rocks 60018 and 65315: Acquisition of terrestrial krypton and xenon indicating an irreversible adsorption process. *Geochim. Cosmochim. Acta* **56**, 493-509.

Okada A., Keil K., Taylor G. J., and Newsom H. (1988) Igneous history of the aubrite parent asteroid: Evidence from the Norton County aubrite. *Meteoritics* **23**, 59-74.

Okazaki R., Nakamura T., Takaoka N., and Nagao K. (2003) Noble gases in ureilites released by crushing. *Meteorit. Planet. Sci.* **38**, 767-781.

Ott U. (2002) Noble gases in meteorites - trapped components. In *Reviews in Mineralogy & Geochemistry*, **47**, 71-100.

Ozima M. and Podosek F.A. (2002) *Noble Gas Geochemistry, 2nd ed*., 286 p., Cambridge Univ. Press, Cambridge.

Podosek F. A. (1970) Dating of meteorites by the high-temperature release of iodine-correlated Xe^{129}. *Geochim. Cosmochim. Acta* **34**, 341-365.

Podosek F. A. (1972) Gas retention chronology of Petersburg and other meteorites. *Geochim. Cosmochim. Acta* **36**, 755-772.

Podosek F.A. and Swindle T. D. (1988) Extinct radionuclides. In *Meteorites and the early solar system* (eds. J. F. Kerridge and M. S. Matthews). The University of Arizona Press, Arizona. pp. 1093-1113.

Rowe M W. and Bogard D. D. (1966) Isotopic composition of xenon from Ca-poor achondrites. *J. Geophys. Res.* **71**, 4183-4188.

Rubin A. E. (1983) Impact melt-rock clasts in the Hvittis enstatite chondrite breccia: Implications for a

genetic relationship between EL chondrites and aubrites. *Proc. Lunar Planet. Sci. Conf.* **14**, B293-B300.

Scherer P. and Schultz L. (2000) Noble gas record, collisional history, and paring of CV, CO, CK and other carbonaceous chondrites. *Meteorit. Planet. Sci.* **35**, 145-153.

Schultz L. and Freundel M. (1985) On the production rate of ^{21}Ne in ordinary chondrites. In *Isotopic ratios in the solar system* (ed. Centre National d'Etudes Spatiales). Cepadues editions, Toulouse. pp. 27-33.

Smith S. P. and Huneke J. C. (1975) Cosmogenic neon produced from sodium in meteoritic minerals. *Earth Planet. Sci. Lett.* **27**, 191-199.

Takaoka N. and Nagao K. (1980) Mass spectrometrical study of rare gas compositions and neutron capture effects in Yamato-74191(L3) chondrite. *Z. Naturforschung* **35a**, 29-36.

Verkouteren R. M. and Lipschutz M. E. (1983) Cumberland Falls chondritic inclusions - II. Trace element contents of forsterite chondrites and meteorites of similar redox state. *Geochim. Cosmochim. Acta* **47**, 1625-1633.

Wacker J. F., Zadnik M. G., and Anders E. (1985) Laboratory simulation of meteoritic noble gases. I. Sorption of xenon on carbon: Trapping experiments. *Geochim. Cosmochim. Acta* **49**, 1035-1048.

Wanless R. K. and Thode H. G. (1955) The fission yields of isotopes of xenon and krypton in the neutron fission of U^{235} and U^{238}. *Canadian J. Phys.* **33**, 541-554.

Watters T. H. and Prinz M. (1979) Aubrites: Their origin and relationship to enstatite chondrites. *Proc. Lunar Planet. Sci. Conf.* **10**, 1073-1093.

Welten K. C., Nishiizumi K., Caffee M. W., and Masarik J. (2002) Cosmogenic radionuclides in aubrites - constraining 2π and 4π exposure histories. *Lunar Planet. Sci*. **XXXIII**. Lunar Planet. Inst., Houston. #5105 (abstr.).

Welten K. C., Nishiizumi K., Hillegonds D. J., Caffee M. W., and Masarik J. (2004) Unraveling the exposure histories of aubrites. *Meteorit. Planet. Sci.* **39**, A113 (abstr.).

Whitby J. A., Gilmour J. D., Turner G., Prinz M., and Ash R D. (2002) Iodine-Xenon dating of chondrules from the Qingzen and Kota Kota enstatite chondrites. *Geochim. Cosmochim. Acta* **66**,

347-359.

Wolf R., Ebihara M., Richter G., and Anders E. (1983) Aubrites and diogenites: Trace element clues to their origin. *Geochim. Cosmochim. Acta* **47**, 2257-2270.

Yang J., Lewis R. S., and Anders E. (1982) Sorption of noble gases by solid, with reference to meteorites. I. Magnetite and carbon. *Geochim. Cosmochim. Acta* **46**, 841-860.

Zähringer J. (1968) Rare gases in stony meteorites. *Geochim. Cosmochim. Acta* **32**, 209-237.

Table 1. List of the measured aubrite samples, and the obtained noble gas concentrations and isotopic ratios.

Sample name	run #	Source (sub #)	Condition of analyses: Weight (g)	Number of steps: crush	Number of steps: heat	^{4}He	^{3}He/^{4}He	^{20}Ne	^{20}Ne/^{22}Ne	^{21}Ne/^{22}Ne	^{40}Ar	^{38}Ar/^{36}Ar	^{40}Ar/^{36}Ar	^{84}Kr	^{132}Xe
Bishopville	#1		0.2384	3	4	8320	0.14689 ± 0.00083	272	0.8196 ± 0.0010	0.8839 ± 0.0020	36600	0.9065 ± 0.0084	6370 ± 182	95.3	6.34
Cumberland Falls	#1	}	0.1460	-	2	2940	0.09237 ± 0.00045	228	0.8256 ± 0.0007	0.9136 ± 0.0011	3010	0.8253 ± 0.0017	487.1 ± 0.6	8.53	2.51
	#2	}	0.3710	3	4	2640	0.09969 ± 0.00184	213	0.8251 ± 0.0009	0.9134 ± 0.0011	2220	0.8919 ± 0.0022	499.3 ± 1.6	12.8	2.62
	#3	USNM (604)	0.0792	-	2	3380	0.09681 ± 0.00176	270	0.8234 ± 0.0011	0.9124 ± 0.0022	10500	0.4213 ± 0.0011	386.6 ± 0.6	77.2	58.0
	#4		0.0230	-	2	2360	0.10351 ± 0.00089	255	0.8349 ± 0.0017	0.9200 ± 0.0021	61200	0.2975 ± 0.0040	1674 ± 60	176	19.9
Mayo Belwa	#1		0.1416	-	2	16900	0.10639 ± 0.00070	448	0.8032 ± 0.0005	0.8793 ± 0.0010	94000	1.0864 ± 0.0025	5146 ± 10	158	8.10
Mt. Egerton	#1	}	0.1145	-	1	716	0.22810 ± 0.00310	98.7	0.8458 ± 0.0013	0.8962 ± 0.0016	3230	0.3261 ± 0.0009	320.1 ± 0.4	303	32.3
	#2	}	0.1971	-	4	961	0.20491 ± 0.00044	124	0.8639 ± 0.0046	0.9138 ± 0.0031	1900	0.4107 ± 0.0011	317.9 ± 0.4	159	14.9
Norton County	#1	}	0.2209	-	2	13000	0.18032 ± 0.00286	564	0.8328 ± 0.0012	0.9082 ± 0.0021	1270	1.2879 ± 0.0024	63.93 ± 0.12	107	4.40
	#2	}	0.3978	3	4	14300	0.19356 ± 0.00116	661	0.8337 ± 0.0010	0.9054 ± 0.0020	655	1.3753 ± 0.0020	45.30 ± 0.05	38.0	3.13
	#3		0.1546	-	2	19300	0.15289 ± 0.00086	720	0.8366 ± 0.0008	0.9045 ± 0.0015	6100	1.3657 ± 0.0030	687.8 ± 1.2	43.4	9.32
Peña Blanca Spring	#1	}	0.2107	-	2	7130	0.18574 ± 0.00285	246	0.8191 ± 0.0007	0.8603 ± 0.0011	3130	0.7776 ± 0.0020	697.9 ± 1.0	64.1	3.24
	#2	}	0.3511	3	4	14600	0.07839 ± 0.00056	215	0.8178 ± 0.0007	0.8584 ± 0.0013	7240	0.7308 ± 0.0013	958.8 ± 2.2	72.7	6.49
	#3		0.0932	-	2	7570	0.19787 ± 0.00108	321	0.8133 ± 0.0007	0.8605 ± 0.0015	2160	0.8872 ± 0.0022	540.4 ± 1.0	87.6	17.7
	#4	USNM (1451)	0.1016	-	2	8800	0.17268 ± 0.00074	316	0.8175 ± 0.0009	0.8705 ± 0.0016	6550	0.8483 ± 0.0027	1503.8 ± 3.0	69.4	10.7
	#5		0.0640	-	2	9370	0.13972 ± 0.00054	291	0.8268 ± 0.0011	0.8745 ± 0.0020	13200	0.5621 ± 0.0119	1405 ± 40	75.5	5.40
Shallowater	#1	USNM (1206)	0.0725	-	2	2280	0.20592 ± 0.00295	94.0	0.8432 ± 0.0010	0.8638 ± 0.0016	4370	0.1865 ± 0.0004	20.05 ± 0.04	937	283
ALHA 78113	#1	NASA (65)	0.1569	-	2	3340	0.12355 ± 0.00023	129	0.8509 ± 0.0060	0.9217 ± 0.0043	1270	0.6604 ± 0.0021	966.9 ± 1.6	44.7	8.69
LAP 02233	#1	NASA (6)	0.1671	-	2	8040	0.16541 ± 0.00045	270	0.8246 ± 0.0058	0.8486 ± 0.0040	1040	1.2052 ± 0.0040	417.52 ± 0.78	69.3	19.4

Concentrations of He, Ne and Ar are given in the unit of 10^{-9} cm^{3}STP/g, and those of Kr and Xe are in 10^{-12} cm^{3}STP/g, respectively.
Cumberland Falls #1 and #2, Mt. Egerton #1 and #2, Norton County #1 and #2, and Pena Blanca Spring #1 and #2 are taken from the same aliquot, respectively.
- Crushing extraction was not applied.

Table 2. Oxygen isotopic compositions in aubrites.

Sample	Note [a]	Weigh (mg)	$\delta^{17}O_{SMOW}$ [b] (‰)	$\delta^{18}O_{SMOW}$ [b] (‰)	$\Delta^{17}O$ [c] (‰)
Cumberland Falls	#3	2.96	3.10	5.30	0.34
	#4	1.89	2.74	5.39	-0.06
	#4	0.70	2.36	4.54	0.00
Peña Blanca Spring	#1, #2	1.86	2.78	5.33	0.01
	#3	2.51	2.80	5.16	0.12
	#4	2.72	2.80	5.18	0.11
	#5	2.09	2.68	5.06	0.05
Shallowater	#1	2.55	2.97	5.59	0.07
ALHA 78113	#1	2.05	2.67	5.27	-0.07
	#1	2.11	2.77	5.22	0.06
	#1	2.17	2.53	4.81	0.03
LAP 02233	#1	2.50	2.74	5.16	0.06
	#1	2.11	2.79	5.25	0.06

[a] Sample is taken from the same specimen for noble gas analysis.

[b] δ notation is defined by $\delta = \{ ({}^{m}O/{}^{18}O)_{sample} / ({}^{m}O/{}^{18}O)_{SMOW} - 1 \} \times 1000$.

[c] $\Delta^{17}O = \delta^{17}O - 0.52 \times \delta^{18}O$ (Clayton, 1993).

Table 3. Cosmogenic noble gases, production rates and cosmic-ray exposure ages for aubrites.

Sample		Cosmogenic noble gases						Production rates		Cosmic-ray exposure ages					
		^{3}He	^{21}Ne	^{38}Ar	^{81}Kr	^{83}Kr	^{126}Xe	P_3	P_{21}	T_3	T_{21}	T_{81} [a]	T_{exp} (Ma)		
		10^{-9}cm^{3}STP/g			10^{-12}cm^{3}STP/g			10^{-9}cm^{3}STP/g/Ma		Ma			obtained [b]	ref [c]	best estimates [d]
Bishopville	#1	1220	294	4.70	0.085	25	0.25	17.4	4.37	70.1	67.3	52±3	52± 3	52.0	52± 3
Cumberland Falls	#1	272	253	4.48	0.0044	1.4	0.074	17.4	5.20	15.7	48.7	46±12	49±10	60.9	49±10
	#2	263	235	3.56	0.0040	1.4	0.045	17.4	5.19	15.1	45.3	51±16			
	#3	327	300	7.72 [e]	<0.035	3.2	0.089	17.4	5.16	18.8	58.1				
	#4	244	281	4.56	n.d.	21	0.19	17.4	5.42	14.0	51.8				
Mayo Belwa	#1	1800	490	18.7	0.057	39	0.93	17.4	4.49	103	109	117±14	117±14	117	117±14
Mt. Egerton	#1	163	105	1.58	<0.002	<0.49	<0.0084	16.3	3.90	10.0	26.9		29±4	26.9	28±4
	#2	197	131	1.52	<0.015	0.045	<0.0070	16.4	4.37	12.0	30.0				
Norton County	#1	2350	615	24.8	<0.003	0.60	0.018	17.4	5.29	135	116		144±19	111	121±16
	#2	2760	718	19.5	<0.003	0.51	0.015	17.4	5.20	158	138	(113±69)			
	#3	2940	778	11.9	<0.007	2.2	0.057	17.4	5.17	169	150				
Peña Blanca Spring	#1	1320	258	3.01	<0.003	<0.46	0.13	17.2	3.79	76.7	68.1		77±10	72.1	75±11
	#2	1150	226	4.66	0.0059	2.0	0.30	17.2	3.74	66.9	60.4	(63±22)			
	#3	1500	340	3.18	<0.004	0.45	0.062	17.2	3.78	87.2	89.9				
	#4	1520	337	3.27	<0.014	1.6	0.16	17.3	3.99	87.9	84.5				
	#5	1309	308	4.01	n.d.	3.7	0.26	17.3	4.08	75.7	75.5				
Shallowater	#1	469	96.3	n.a.	<0.015	<3.1	<0.053	16.5	3.35	28.4	28.7		29±4	27.0	28±4
ALHA 78113	#1	431	139	1.65 [e]	<0.005	0.37	<0.012	17.6	5.57	24.5	25.0		25±4	21.1	23±4
LAP 02233	#1	1330	278	2.89	<0.008	0.50	0.042	17.1	3.57	77.8	77.9		78±12		78±12

[a] T_{81} (^{81}Kr-Kr age) and cosmogenic Kr data are given in Table 4. T_{81} for Norton County and Pena Blanca Spring is not used for calculation of T_{exp}.

[b] Cosmic-ray exposure ages obtained using the measured noble gas data (T_{81}, T_{21} or average of T_3 and T_{21}; criterion is mentioned in text).

[c] Cosmic-ray exposure ages given in Lorenzetti et al. (2003).

[d] Cosmic-ray exposure ages we recommend to be most reliable.

[e] Low temperature fraction is excluded.

n.d. Not determined.

n.a. Not available, since cosmogenic Ar is masked by Ar from neutron capture of Cl and trapped Ar.

Table 4. Cosmogenic Kr (including neutron induced Kr) and ^{81}Kr-Kr ages in aubrites.

Sample		Temp.[a] °C	Fraction[a] of $(^{83}Kr)_c$	$(^{83}Kr)_c$ $10^{-12}cm^3/g$	^{78}Kr	^{80}Kr[b]	^{81}Kr	^{82}Kr[b]	^{84}Kr	P_{81}/P_{83}[c]	^{81}Kr-Kr age[d] Ma
					^{83}Kr = 1						
Bishopville	#1	1000 +1400	0.96	24.1	0.142 ± 0.006	0.555 ± 0.027	0.0033 ± 0.0002	0.76 ± 0.04	0.74 ± 0.05	0.561 ± 0.008	52 ± 3
Cumberland Falls	#1	1800	0.84	1.20	0.136 ± 0.013	2.150 ± 0.182	0.0037 ± 0.0010	1.14 ± 0.14	0.76 ± 0.30	0.553 ± 0.016	46 ± 12
	#2	1000 +1400	0.77	1.23	0.092 ± 0.005	0.936 ± 0.029	0.0030 ± 0.0009	0.77 ± 0.03	0.67 ± 0.06	0.497 ± 0.006	51 ± 16
Mayo Belwa	#1	1800	1.0	38.6	0.142 ± 0.005	0.685 ± 0.023	0.0015 ± 0.0002	0.82 ± 0.03	0.77 ± 0.06	0.560 ± 0.007	117 ± 14
Norton County	#2	1400	0.75	0.382	0.154 ± 0.011	0.580 ± 0.026	0.0016 ± 0.0010	0.76 ± 0.05	0.77 ± 0.16	0.576 ± 0.014	113 ± 69
Peña Blanca Spring	#2	1000 +1400 +1800	0.97	1.91	0.183 ± 0.005	0.694 ± 0.016	0.0030 ± 0.0011	0.82 ± 0.05	0.72 ± 0.15	0.612 ± 0.006	63 ± 22

[a] Temperature steps used for ^{81}Kr-Kr age determinations, and fractions of $(^{83}Kr)_c$ released at these temperatures.

[b] Kr produced from neutron captures on Br is also included in some samples (see text).

[c] $P_{81}/P_{83} = 1.262(^{78}Kr/^{83}Kr)_c+0.381$ (Marti and Lugmair, 1971).

[d] $T_{81}=(1/\lambda_{81})(P_{81}/P_{83})(^{83}Kr/^{81}Kr)_c$, where λ_{81} is the decay constant of ^{81}Kr (Eugster et al. 1967; Marti, 1967).

Table 5. Noble gases produced from neutron captures in aubrites.

Sample		$(^{80}Kr)_n$[a] $10^{-12}cm^3/g$	$(^{80}Kr/^{82}Kr)_n$[a]	$(^{128}Xe)_n$ $10^{-12}cm^3/g$	$(^{128}Xe/^{80}Kr)_n$	$(^{36}Ar)_n$ $10^{-9}cm^3/g$	$(^{36}Ar/^{80}Kr)_n$
Bishopville	#1	0.8	1.46±0.34[b]	<0.05	<0.06	-	-
Cumberland Falls	#1	2.3	4.3±1.3[c]	(0.027)	(0.012)	-	-
	#2	0.7	3.0±1.2[c]	(0.005)	(0.007)	-	-
	#3	28	2.70±0.09[c]	0.76	0.027	>2.3	>82
	#4	199	2.74±0.19[c]	0.24	0.0012	>0.31	>1.9
Mayo Belwa	#1	4.9	2.4±1.7[c]	0.35	0.071	-	-
Mt. Egerton	#1	<0.4	-	<0.02	-	-	-
	#2	<0.3	-	<0.02	-	-	-
Norton County	#1	<0.2	-	<0.02	-	-	-
	#2	<0.2	-	<0.01	-	-	-
	#3	<0.04	-	<0.04	-	-	-
Peña Blanca Spring	#1	0.4	-	<0.05	<0.2	-	-
	#2	0.3	-	<0.06	<0.2	-	-
	#3	<0.3	-	<0.02	-	-	-
	#4	<0.2	-	<0.05	-	-	-
	#5	0.4	-	<0.04	<0.1	-	-
Shallowater	#1	15	2.71±0.78[b]	0.42	0.028	>0.64	>41
ALHA 78113	#1	1.2	2.63±0.61[c]	<0.01	<0.01	>0.14	>120
LAP 02233	#1	<0.2	-	<0.04	-	-	-

[a] Cosmogenic Kr is corrected (fraction of neutron capture Kr is 74 - 94 % and 32 -84 % of total excesses for ^{80}Kr and ^{82}Kr, respectively).

[b] 600 ºC fraction.

[c] 1800 ºC fraction.

- Significant data could not be obtained.

Although data in parentheses have large experimental errors, we consider them to be reasonable by comparing with data of the other specimens for Cumberland Falls (see text).

Table 6. Radiogenic ^{129}Xe and fission Xe in aubrites.

Sample		Total amounts [a]		Temperature fractions where significant radiogenic and fission Xe were observed					
		$(^{129}Xe)_{rad}$	$(^{136}Xe)_{fiss}$	Temp	^{136}Xe	^{129}Xe	^{131}Xe	^{132}Xe	^{134}Xe
		$10^{-12}cm^3/g$		ºC	$10^{-12}cm^3/g$	$^{136}Xe = 1$			
Bishopville	#1	$0.71^{+0.33}_{-0.24}$	<0.08						
Cumberland Falls	#1	1.5±0.1	$0.54^{+0.08}_{-0.06}$	1800	0.54±0.06	2.68±0.45	0.51±0.31	1.02±0.24	0.95±0.16
	#2	$0.56^{+0.15}_{-0.08}$	$0.45^{+0.07}_{-0.06}$	1400	0.22±0.02	1.25±0.26	0.48±0.28	1.11±0.20	0.94±0.13
				1800	0.19±0.02	1.21±0.23	0.35±0.16	1.06±0.17	0.95±0.13
	#3	46.6±2.3	$0.31^{+0.41}_{-0.30}$						
	#4	21.8±1.1	$1.12^{+0.31}_{-0.18}$	1800	1.12±0.18	18.8±3.2	0.72±0.49	1.01±0.43	1.04±0.27
Mayo Belwa	#1	7.4±1.0	0.35±0.13	1800	0.35±0.13	20.1±6.4	-1.1±1.2	1.70±1.11	0.97±0.45
Mt. Egerton	#1	<0.38	<0.27						
	#2	<0.08	<0.18						
Norton County	#1	$0.28^{+0.16}_{-0.06}$	<0.08						
	#2	$0.22^{+0.09}_{-0.07}$	<0.08						
	#3	0.43±0.11	<0.19						
Peña Blanca Spring	#1	35.8±1.8	<0.02						
	#2	42.9±2.1	$0.44^{+0.22}_{-0.14}$	1000	0.05±0.01	25.4±6.7	-1.0±1.2	1.14±0.64	0.89±0.33
				1400	0.30±0.03	61.6±5.4	-0.7±1.0	1.22±0.34	0.86±0.11
	#3	12.3±0.6	<0.05						
	#4	12.7±0.6	<0.04						
	#5	39.4±1.5	<0.08						
Shallowater	#1	461±23	<0.69						
ALHA 78113	#1	$0.46^{+0.06}_{-0.05}$	$0.14^{+0.08}_{-0.05}$	1800	0.14±0.06	3.3±1.8	<1.3	<2.3	1.05±0.67
LAP 02233	#1	$0.23^{+0.20}_{-0.15}$	$0.16^{+0.17}_{-0.09}$	1800	0.16±0.09	1.5±1.5	<1.1	<2.0	0.76±0.68
^{244}Pu fission [b]						0.048±0.055	0.246±0.015	0.885±0.030	0.939±0.008
^{238}U fission [c]						<0.001	0.083±0.002	0.570±0.003	0.818±0.003
^{235}U fission [d]							0.453	0.678	1.246
HL [e]						1.511±0.003	1.210±0.002	1.430±0.610	0.909±0.005

[a] Total concentration of all extraction steps (sum of crushing and heating steps in case of available).
[b] Alexander et al. (1971).
[c] Eikenberg et al. (1993).
[d] Wanless and Thode (1955).
[e] Busemann et al. (2000), $^{130}Xe/^{136}Xe$ of Xe-HL is 0.2206 +/- .0004.
- No significant excess is observed beyond the experimental error.

Table 7. Trapped noble gases in aubrites.

Sample		$(^{36}Ar)_t$	$(^{84}Kr)_t$	$(^{132}Xe)_t$	$(^{36}Ar/^{132}Xe)_t$	$(^{84}Kr/^{132}Xe)_t$	Trapped component [a]
		$10^{-9}cm^3/g$	$10^{-12}cm^3/g$				
Bishopville	#1	2.72	76.5	6.21[b]	438	12.3	Air
Cumberland Falls	#1	3.28	7.43	1.89	1735	3.93	Chondritic[c]
	#2	2.15	11.6	2.07	1039	5.60	Chondritic[c]
	#3	22.6	74.1	57.5	393	1.29	Chondritic[c]
	#4	33.6	155	18.5	1816	8.38	Chondritic[c]
Mayo Belwa	#1	6.21	130	6.56[b]	947	19.8	Air
Mt. Egerton	#1	9.05	303[b]	32.0	283	9.47	Air
	#2	5.00	159[b]	14.9[b]	336	10.7	Air
Norton County	#1	3.81	107	4.31	884	24.8	Air
	#2	1.86	37.4	3.08	604	12.1	Air
	#3	1.20	41.4	9.09	132	4.55	Air
Peña Blanca Spring	#1	2.54	64.1[b]	3.24[b]	784	19.8	Air
	#2	4.54	71.2	5.72	794	12.4	Air+Chondritic[c]
	#3	1.95	86.7	17.7[b]	110	4.90	Air
	#4	2.24	67.7	10.7[b]	209	6.33	Air
	#5	6.83	73.0	5.27	1296	13.9	Air+Chondritic[c]
Shallowater	#1	218	937[b]	283[b]	770	3.31	Air+Chondritic[c]
ALHA 78113	#1	2.00	44.1	8.54	234	5.16	Air+Chondritic[c]
LAP 02233	#1	0.633	68.9	19.3	32.8	3.57	Air

[a] Major trapped constituent estimated based on Ar/Kr/Xe elemental ratios (*cf*. Fig. 6), which is used for decomposition of measured noble gases into cosmogenic, trapped and nucleogenic components.

[b] All measured Kr or Xe seems to be of trapped origin (see text).

[c] Ar/Kr/Xe elemental ratios are close to those of South Oman (Ar-rich relative to Q) or between Q and South Oman.

Figure captions

Fig. 1. Oxygen isotope plot of $\delta^{17}O$ vs. $\delta^{18}O$ for the measured aubrites. Typical areas for aubrites (Clayton and Mayeda, 1996; Newton et al., 2000), other achondrites (HEDs and SNCs; Clayton and Mayeda, 1996), and L and LL chondrites (Clayton, 2003) are given for comparison. The "TF line" is the terrestrial mass fractionation line calculated from the equation of $\delta^{17}O = 0.52 \times \delta^{18}O$ (Clayton, 1993). The analytical accuracy of $\delta^{17}O$ and $\delta^{18}O$ is approximately 0.1‰.

Fig. 2. Distribution of cosmic-ray exposure ages of aubrites is shown with neutron fluences determined based on neutron capture Sm, in addition to sample characteristics (breccia or not, with/without solar wind noble gases, with/without a neutron-capture-produced noble gas nuclides and with/without chondritic noble gas signatures). Multiple break-up events, possibly 4-9 (indicated by right side bars) except for anomalous aubrites of Mt. Egerton and Shallowater, are considered to have occurred on the aubrite parent body. It has been reported that Mt. Egerton might be a sample of mantle-core boundary of the aubrite parent body and that Shallowater might have originated from a different parent body. Data sources: this work and Lorenzetti et al. (2003) for cosmic-ray exposure ages, and Hidaka et al. (1999) and Hidaka et al. (2005) for neutron fluences. See Table 3 for the adopted cosmic-ray exposure ages of the nine aubrites studied in this work.

Fig. 3. $^{80}Kr/^{84}Kr$ vs. $^{82}Kr/^{84}Kr$ for aubrites. Measured data (symbols shown in the legend) and data from references (small solid circles) are shown. Numerals next to symbols denote gas extraction temperatures in 100°C and sample numbers in parentheses. The terrestrial atmospheric Kr (Ozima and Podosek, 2002), Q-Kr (Busemann et al., 2000), directions towards cosmogenic Kr for aubrites (Busemann and Eugster, 2002) and Kr produced from neutron captures on Br at the epithermal neutron energy range of 30-300 eV ($(^{80}Kr/^{82}Kr)_n = 2.62$; Marti et al., 1966) are shown. The figure shows that the majority of excess Kr can be assigned as either cosmogenic Kr (e.g., 1000 and 1400°C of Bishopville, Mayo Belwa and some data of Peña Blanca Spring), Kr produced from neutron captures on Br (e.g. some data of Cumberland Falls and 600°C of

Shallowater) or a mixture of these components. References for Kr data of aubrites: Eugster et al. (1969) for Khor Temiki, and Lorenzetti et al. (2003) for Cumberland Falls, Mayo Belwa, Mt. Egerton and Shallowater. Abbreviations are shown for some reference data with remarkable cosmogenic or neutron capture Kr shifts: KT, Khor Temiki; MB, Mayo Belwa.

Fig. 4. $^{124}Xe/^{130}Xe$ vs. $^{126}Xe/^{130}Xe$ for aubrites. Measured data (symbols shown in the legend) and data from references (small solid circles) are shown. Numerals next to symbols are gas extraction temperatures in 100°C and sample numbers in parentheses. The terrestrial atmospheric Xe (Ozima and Podosek, 2002), Q-Xe (Busemann et al., 2000), solar wind Xe (Mathew and Mari, 2003), directions of cosmogenic Xe for aubrites (Busemann and Eugster, 2002), and those of light rare earth elements and Ba targets (Hohenberg et al., 1981) are shown. References for Xe data of aubrites: Busemann and Eugster (2002) for Cumberland Falls, Mayo Belwa, Mt. Egerton, Norton County and Shallowater, Eugster et al. (1969) for Khor Temiki, Kim and Marti (1992) for Pesyanoe, Mathew and Mari (2003) for Pesyanoe, and Rowe and Bogard (1966) for Cumberland Falls, Norton County, Peña Blanca Spring and Shallowater. Abbreviations are given for some reference data with remarkable cosmogenic Xe shifts: KT, Khor Temiki; MB, Mayo Belwa; NC, Norton County; PBS, Peña Blanca Spring.

Fig. 5. $^{128}Xe/^{130}Xe$ vs. $^{129}Xe/^{130}Xe$ after cosmogenic correction for the measured aubrites. Numerals next to symbols are gas extraction temperatures in 100°C and sample numbers in parentheses. Data for Cumberland Falls and Shallowater that were reported by Busemann and Eugster (2002), after cosmogenic correction with the manner used in this study, are also shown as small solid circles (labeled respectively as CF and S). The $(^{128}Xe)_n/(^{129}Xe)_{rad}$ ratio is constant within each aubrite in spite of the wide range of the absolute amounts of $(^{128}Xe)_n$ and $(^{129}Xe)_{rad}$ (Tables 5 and 6). The ratios of $(^{128}Xe)_n/(^{129}Xe)_{rad}$ are in the order of Mayo Belwa > Cumberland Falls > Shallowater. The terrestrial atmospheric Xe is taken from Ozima and Podosek (2002) and Q-Xe from Busemann et al. (2000).

Fig. 6. Trapped $^{36}Ar/^{132}Xe$ vs. $^{84}Kr/^{132}Xe$. (a) Data calculated as bulk samples (sum of all crushing and heating steps) for the nine measured aubrites. (b) Data for each crushing and heating step for the

four aubrites with chondritic noble gas signatures, Cumberland Falls, Peña Blanca Spring, Shallowater and ALHA 78113. Numerals that are shown close to or inside symbols show extraction conditions (C, crushing step; 6, 10, 14 and 18, heating temperatures in 100°C) and sample numbers in parentheses. According to this figure, at each temperature step, a major trapped component was identified. The isotopic ratios of terrestrial atmosphere were adopted for the data close to the terrestrial trend, and those of Q were adopted for the data close to the chondritic trend (Q-Kr and Xe were adopted in all temperature steps of Cumberland Falls, 1400 and 1800°C of Peña Blanca Spring #2, 1800°C of Peña Blanca Spring #5, 1800°C of Shallowater and 1800°C of ALHA 78113). The compositions of terrestrial atmospheric Ar, Kr and Xe were taken from Ozima and Podosek (2002). Those of the enstatite chondrite South Oman (as a representative of Ar-rich noble gas composition) were taken from Crabb and Anders (1981), Q were from Busemann et al. (2000), and chondrite area were from Marti (1967b) and Zähringer (1968).

Fig. 7. Isotopic compositions of Xe relative to the terrestrial atmosphere in permil deviation for aubrites with chondritic noble gases. $\delta^{m}Xe = \{ (^{m}Xe/^{132}Xe)_{sample}/(^{m}Xe/^{132}Xe)_{terrestrial\ atmosphere} - 1 \} \times 1000$. Solar Xe observed in Pesyanoe (Mathew and Marti, 2003) and Q-Xe (Busemann et al., 2000) are shown for comparison. (a) $\delta^{m}Xe$ of 1800°C step of Shallowater. (b) $\delta^{m}Xe$ of samples with less contribution of cosmogenic and fission (1000°C of Cumberland Falls #2, 600 and 1800°C of Cumberland Falls #3, 1800°C of Peña Blanca Spring #2 and 1800°C of ALHA 78113). Xe isotopic compositions in Shallowater (plotted on (a)) and 600°C of Cumberland Falls #3 (plotted on (b)) are close to those of Q-Xe. Cumberland Falls #3 contains abundant trapped Xe among the measured specimens, having small contributions of cosmogenic and fission Xe.

Fig. 8. $^{134}Xe/^{130}Xe$ vs. $^{136}Xe/^{130}Xe$ after cosmogenic correction for the measured aubrites. Numerals next to symbols are gas extraction temperatures in 100°C and sample numbers in parentheses. Some data for Cumberland Falls, Mayo Belwa and Peña Blanca Spring demonstrate the presence of ^{244}Pu derived fission Xe. Two data of Peña Blanca Spring (1800°C of #1 and #5) plot near and lower than solar Xe, however, these are probably contributed by cosmogenic Xe from Cs (^{133}Cs is

the only stable isotope of Cs). References for fission Xe and trapped Xe are shown in Table 6 and caption of Fig. 5, respectively.

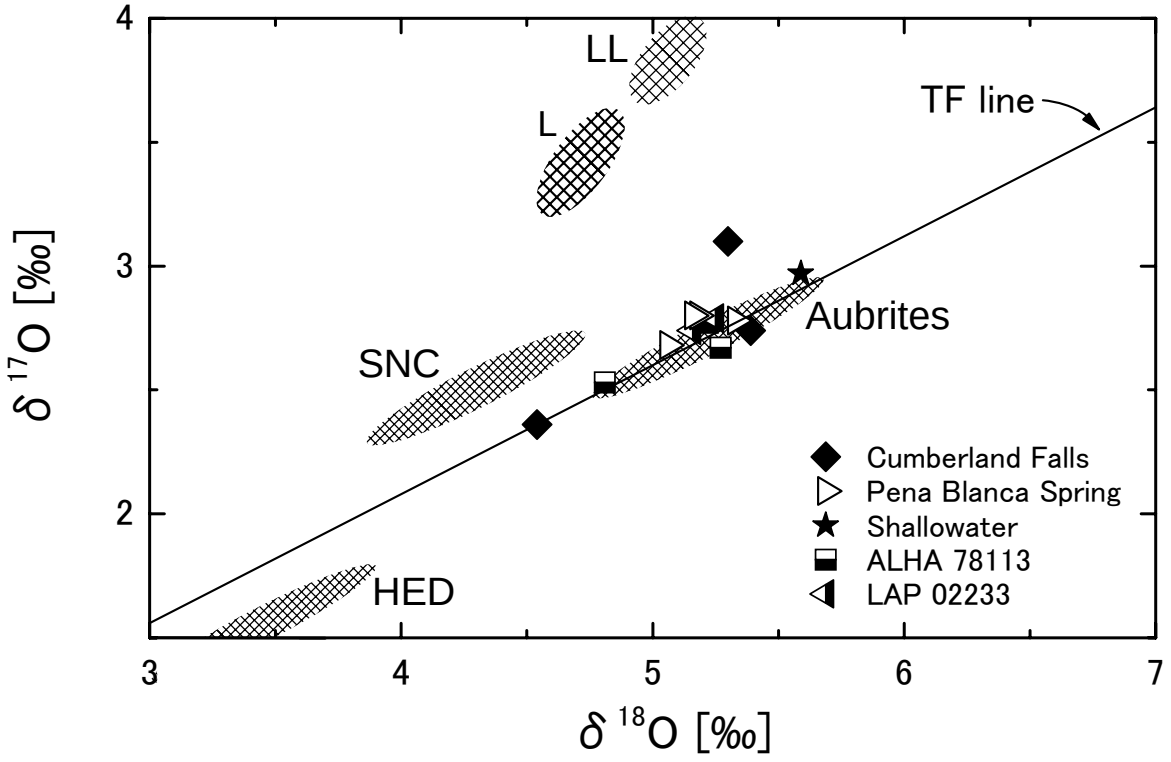

Fig. 1 Miura et al.

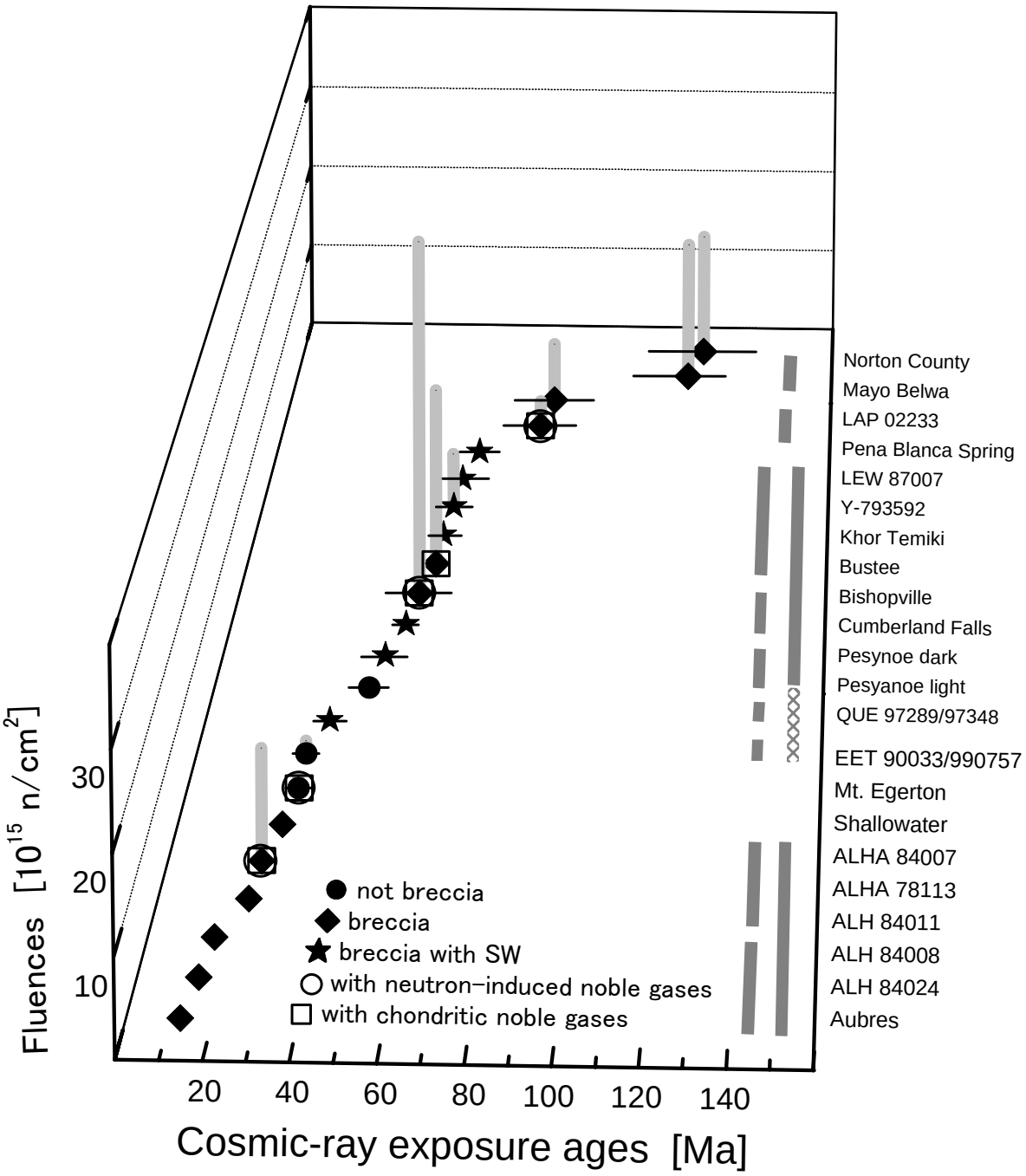

Fig. 2 Miura et al.

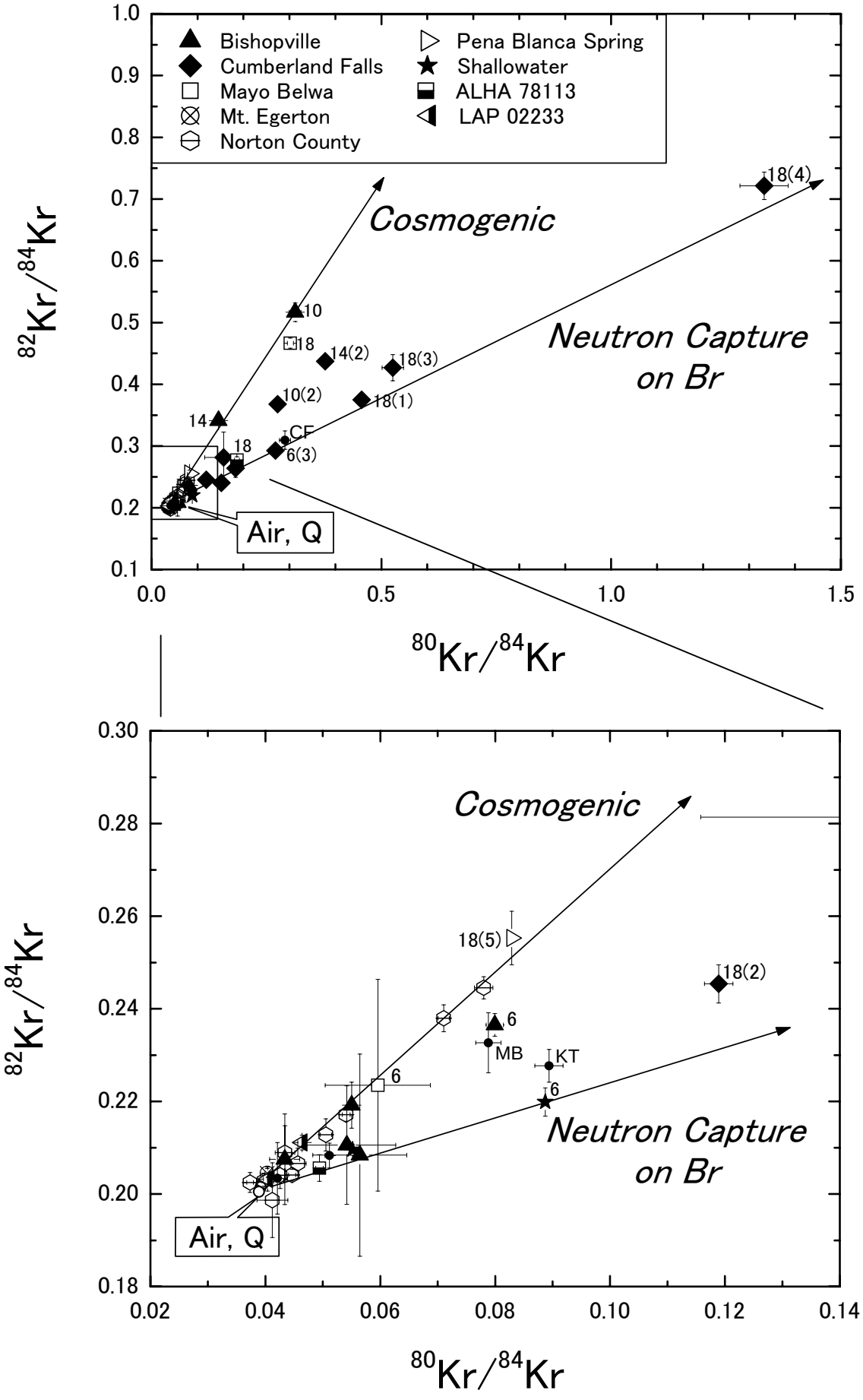

Fig. 3 Miura et al.

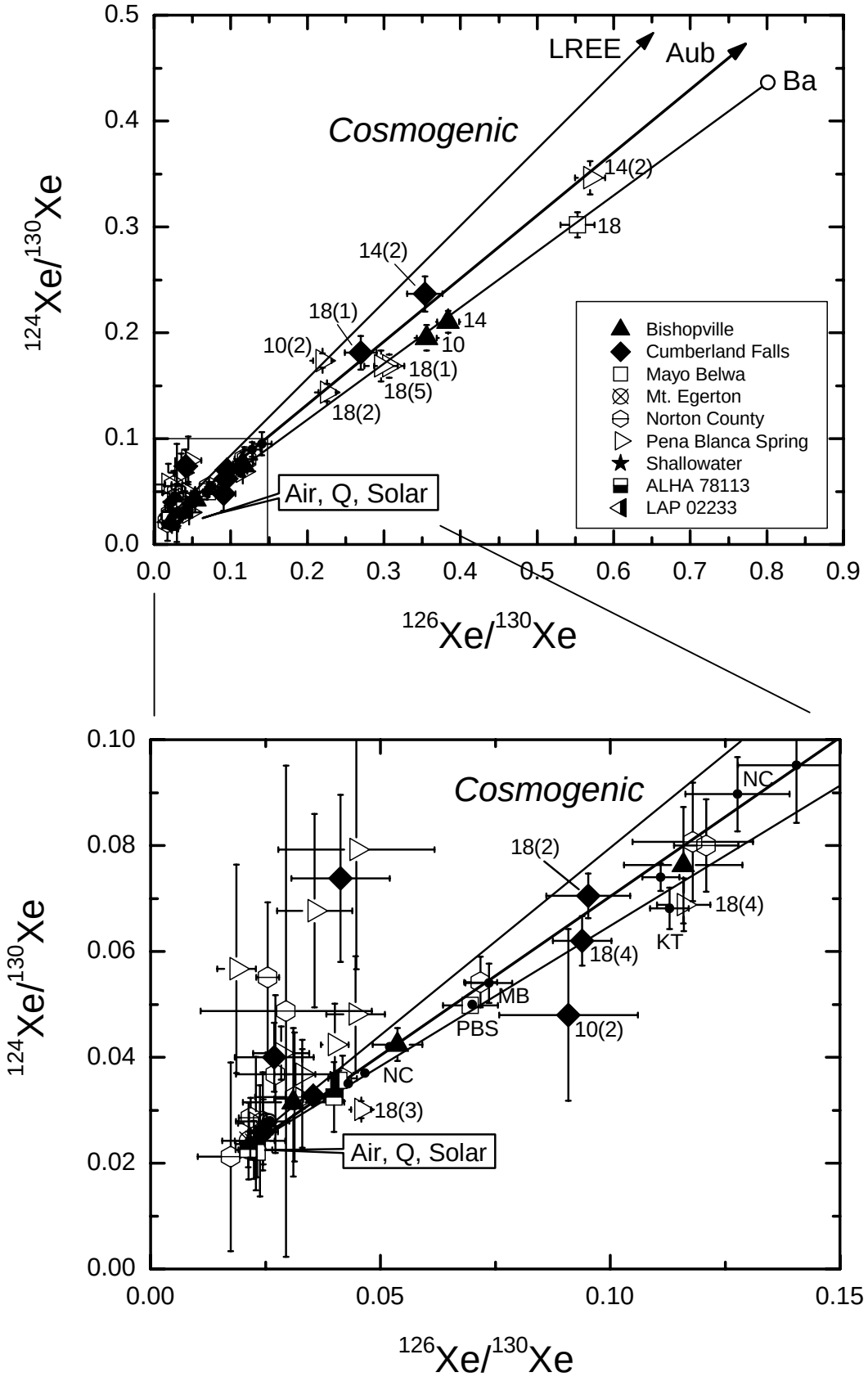

Fig. 4 Miura et al.

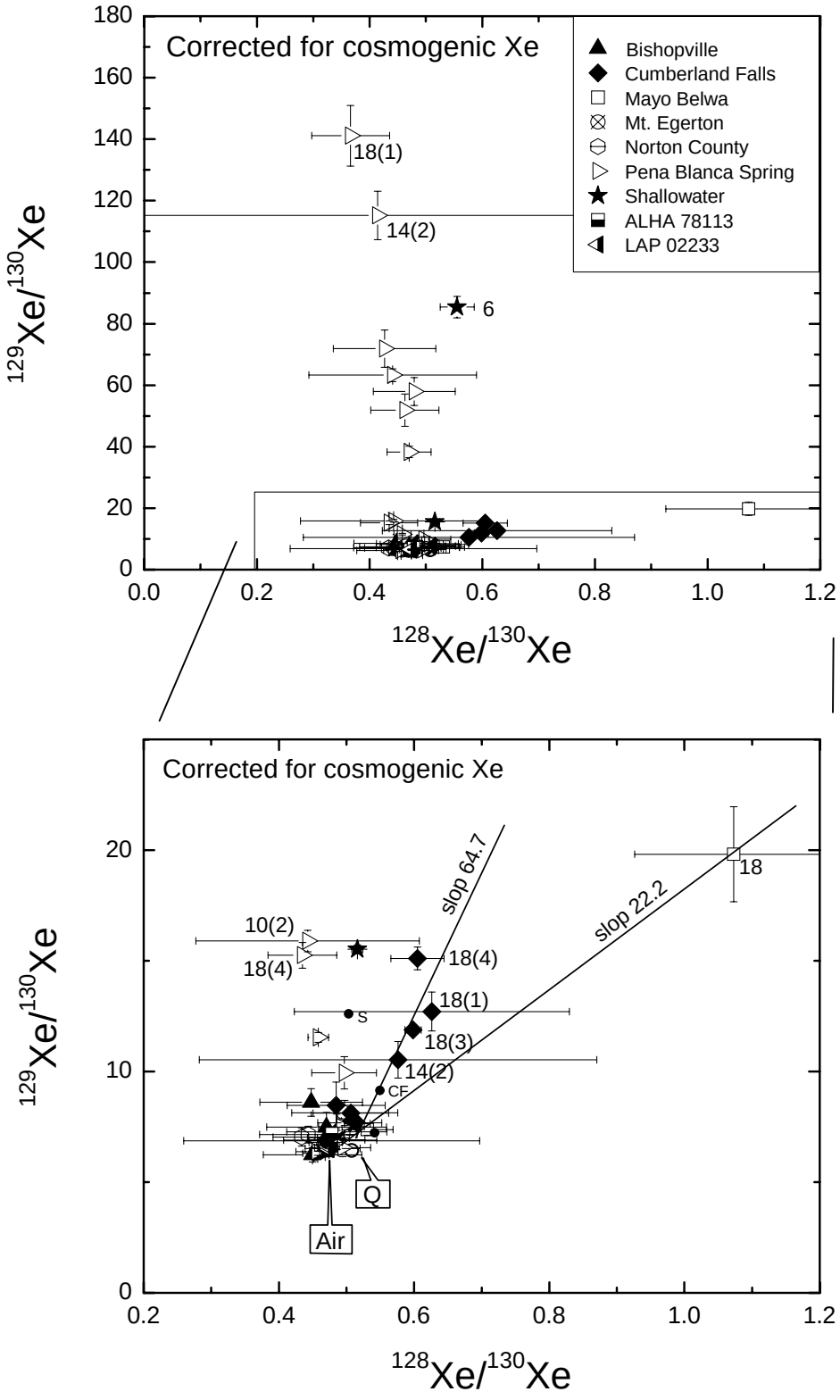

Fig. 5 Miura et al.

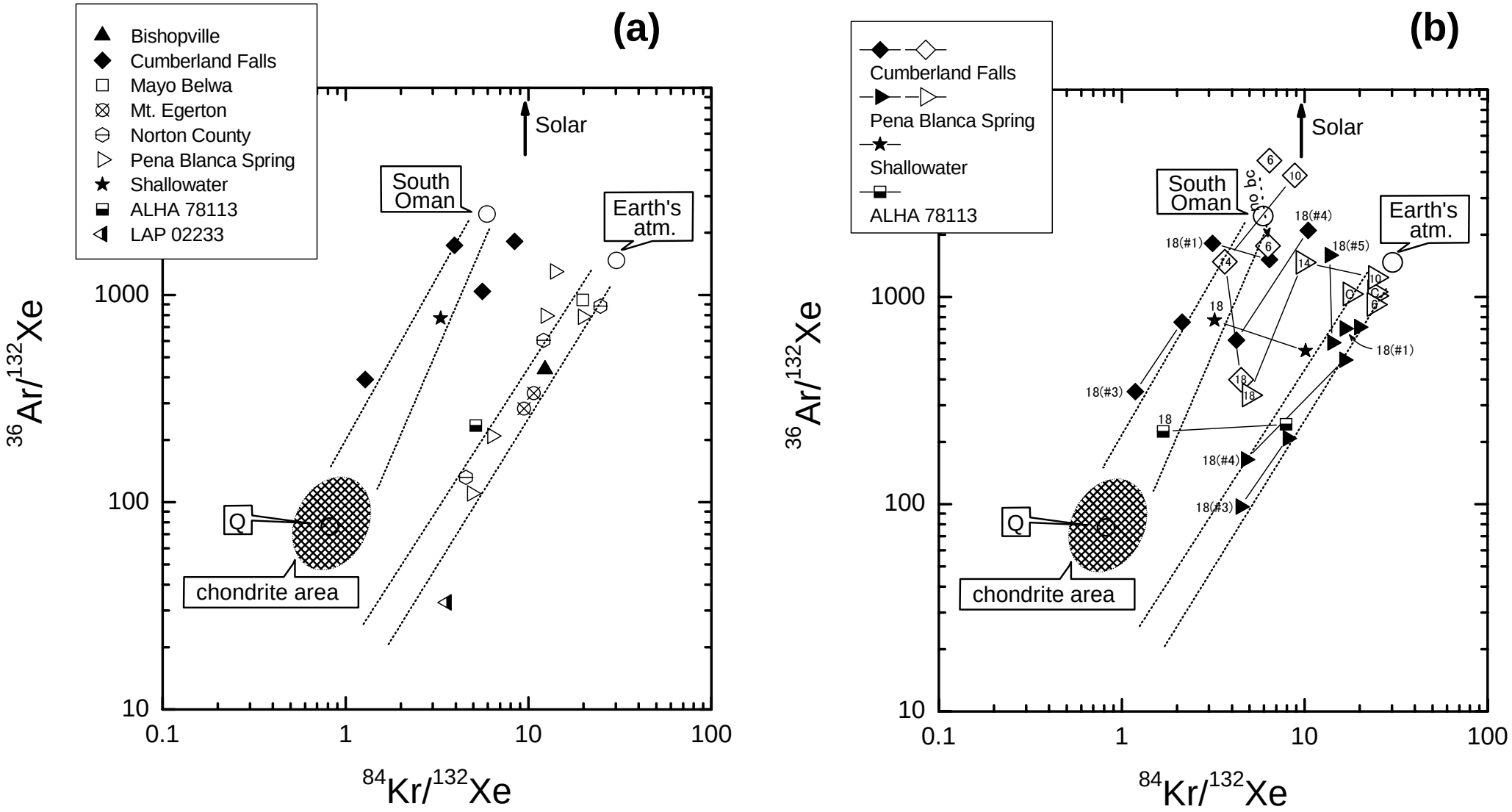

Fig. 6 Miura et al.

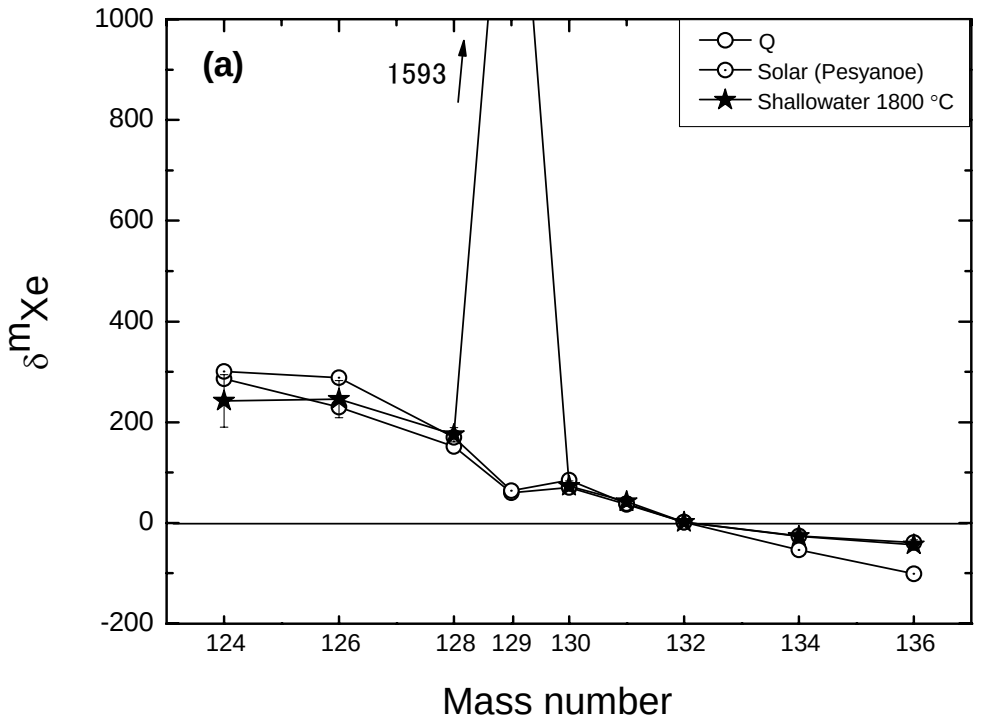

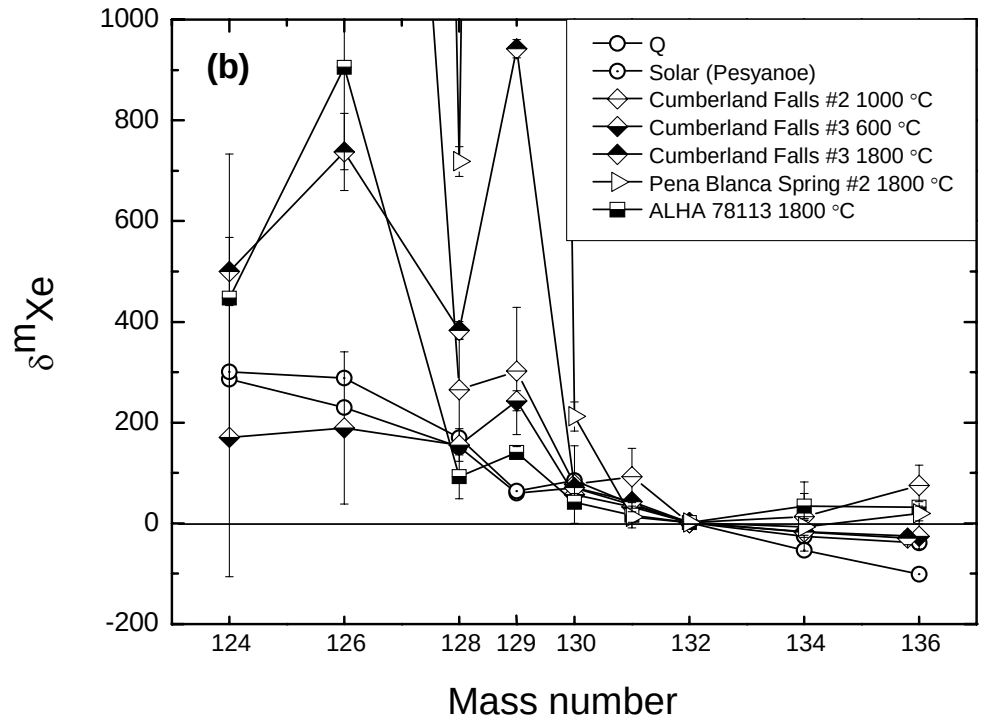

Fig. 7 Miura et al.

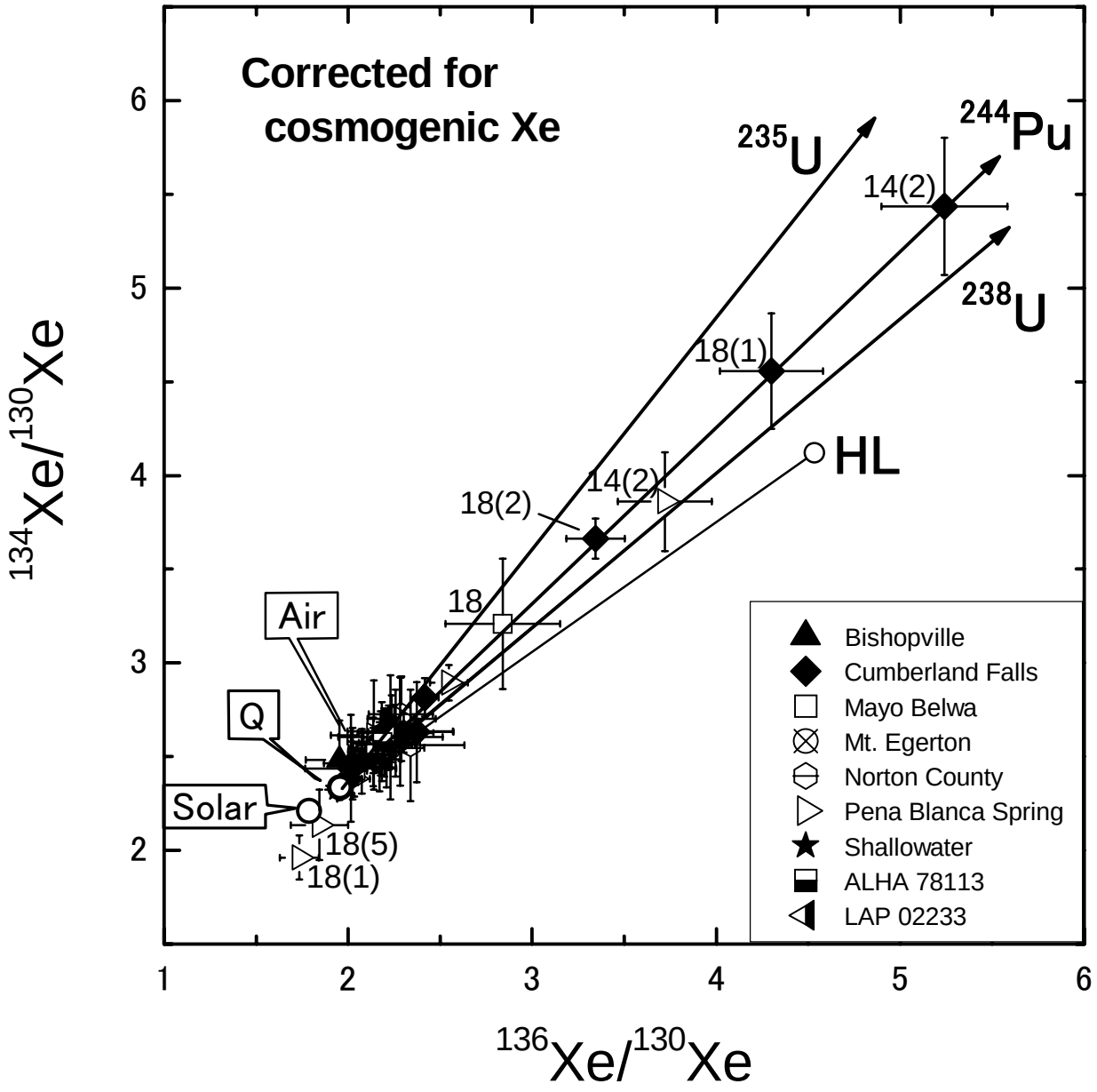

Fig. 8 Miura et al.